REGULATION OF TCR SIGNALING TO NF-κB

by

Suman Paul, M.B.B.S

Dissertation submitted to the Faculty of the
Emerging Infectious Diseases (EID) Graduate Program
Uniformed Services University of the Health Sciences
In partial fulfillment of the requirements for the degree of
Doctor of Philosophy 2013

UNIFORMED SERVICES UNIVERSITY, SCHOOL OF MEDICINE GRADUATE PROGRAMS
Graduate Education Office (A 1045), 4301 Jones Bridge Road, Bethesda, MD 20814

DISSERTATION APPROVAL FOR THE DOCTORAL DISSERTATION IN THE EMERGING INFECTIOUS DISEASES GRADUATE PROGRAM

Title of Dissertation: "Regulation of TCR signaling to NF-kB "

Name of Candidate: Suman Paul
Doctor of Philosophy Degree
March 20, 2013

DISSERTATION AND ABSTRACT APPROVED:

DATE:

3/29/13

Dr. Joseph Mattapallil
DEPARTMENT OF MICROBIOLOGY AND IMMUNOLOGY
Committee Chairperson

3/20/13

Dr. Brian C. Schaefer
DEPARTMENT OF MICROBIOLOGY AND IMMUNOLOGY
Dissertation Advisor

3/20/13

Dr. Edward Mitre
DEPARTMENT OF MICROBIOLOGY AND IMMUNOLOGY
Committee Member

3-20-13

Dr. Michael Schell
DEPARTMENT OF PHARMACOLOGY
Committee Member

Copyright Statement

The author hereby certifies that the use of any copyrighted material in the dissertation manuscript entitled: Regulation of TCR signaling to NF-κB, is appropriately acknowledged and, beyond brief excerpts, is with the permission of the copyright owner.

SUMAN PAUL

ACKNOWLEDGMENTS

Thanks to Brian, for teaching me how to think and write like a scientist

Thanks to Anuj, for showing me how to handle pipettes

Thanks to all Schaefer lab members, past and present

Thanks to the American Heart Association and Henry M Jackson foundation for funding my projects

Thanks to Ron, Derek and Roderick; friends, roommates, and fellow graduate students, for keeping me sane through the last five years

Thanks to my parents for letting me do what I want, and my brother and sister-in-law for dragging me into basic science

ABSTRACT

Regulation of TCR signaling to NF-κB

Suman Paul

Thesis directed by: Brian C Schaefer, Ph.D. Associate Professor,
Department of Microbiology and Immunology

T cells play an important role in the adaptive immune response to invading pathogens. Pathogen derived antigenic peptides in combination with MHC molecules are recognized by the T cell receptor (TCR). Antigen-specific binding initiates signaling cascades in the T cell cytosol that ultimately culminate in the activation of several key transcription factors. One such transcription factor is NF-κB, which controls expression of genes required for T cell activation, proliferation and gain of effector function. The signaling proteins Bcl10 and Malt1 are required for successful transmission of the activation signal from the TCR to NF-κB. Previous observations demonstrated that antigen mediated TCR stimulation leads to formation of Bcl10 and Malt1 cytosolic aggregates, which were named POLKADOTS. Using primary effector T cells and D10 CD4 T cell clones, we demonstrate that the TCR-to-NF-κB activation signal is both transmitted by and terminated at the POLKADOTS signalosome. We show that POLKADOTS formation depends on binding of K63-polyubiquitinated Bcl10 to cytosolic p62 clusters, and that these clusters are the sites of IKK and IκBα phosphorylation, two critical steps required for NF-κB activation. Additionally, we demonstrate that in response to TCR stimulation,

a significant fraction of K63-polyubiquitinated Bcl10 within the POLKADOTS is selectively taken up and degraded by autophagolysosomes. This degradation reduces the amount of actively signaling Bcl10 molecules available for signal transmission, which ultimately limits the degree of NF-κB activation. Thus by both providing a platform for transmission of the activation signal and by degrading the crucial signaling protein Bcl10, POLKADOTS serve as an important cytosolic signal integration site for the TCR-to-NF-κB cascade.

TABLE OF CONTENTS

LIST OF FIGURES

CHAPTER 1: Introduction, Hypothesis and Aims

Parts of this chapter have been published in *Trends in Immunology* as:

"A new look at T cell receptor signaling to nuclear factor kappa B"

Suman Paul[1] and Brian C Schaefer[1,2,*]

[1]Department of Microbiology and Immunology, and [2]Center for Neuroscience and Regenerative Medicine, Uniformed Services University, Bethesda, MD 20814

Epub: March6, 2013. doi: 10.1016/j.it.2013.02.002

T CELLS AND T CELL RECEPTOR SIGNALING

T cells are a type of white blood cells that are present in the blood stream and lymphatics. T cells recognize foreign proteins (referred to as antigens) present on pathogens (virus, bacteria, parasites etc), and mount an immune response designed to clear the invading organisms. The pathogen-derived antigens are taken up and processed by specialized proteases to peptides. These antigenic peptides are displayed by major histocompatibility complex (MHC) molecules on the surface of a specialized group of cells called antigen presenting cells (APCs), which consist of dendritic cells, macrophages, and B cells. T cells utilize a heterodimeric transmembrane receptor, called the T cell receptor (TCR), to scan the peptide antigens displayed by the MHC on the APC surface. Upon specific recognition of a foreign protein-MHC complex on the APC surface, the TCR is stimulated, initiating several cytosolic signaling cascades in the T cells. One such signaling pathway leads to the activation of NF-κB, a transcription factor that controls expression of genes critical for T cell activation and proliferation.

Subsequently, the activated T cells launch an immune response to protect the body from the pathogens.

The T cell response to the pathogens depends on the type of T cells. Broadly, T cells can be classified as CD4+ or CD8+ (cluster of differentiation 4 or 8) cells based on the presence and absence of the cell surface proteins CD4 and CD8. CD8+ cells, also known as cytotoxic cells, recognize antigens bound to cell surface MHC class I molecules. On detection of a MHC I linked foreign peptide (majority originating from cytosolic pathogens, like viruses), activated CD8+ cells secrete enzymes (perforins, granzymes etc) in order to kill the infected cells. CD4+ cells, also known as helper cells (T_H), recognize peptides bound to MHC class II molecules and assist other cells in mounting an immune response. Upon stimulation, CD4+ cells can differentiate into several types of effector cells, each type having a different set of functions. There are at least four well characterized CD4+ effector cell types; T_H1, T_H2, T_H17 and T_{reg} (T regulatory cells). T_H1 cells secrete cytokines (such as INF- γ, TNF-α etc) that activate macrophages allowing them to kill intracellular microbes. T_H2 cells induce B cells to mature into immunoglobulin secreting plasma cells, and also assisting B cells in immunoglobulin class switching. T_H17 cells activate stromal and epithelial cells to produce chemokines that attract neutrophils to infection sites. T_{reg} cells are a mixed group of effector CD4+ cells that secrete cytokines (such as TGF-β, IL-10 etc) and suppress the activity of other T cell types, thereby preventing an unrestricted immune response that might lead to autoimmunity. As NF-$\varkappa$B activation is required for proper T cell function post-TCR stimulation, successful signal transduction from the cell surface TCR to the cytosolic NF-$\varkappa$B is therefore critical in our body's defense against infection.

THE CURRENT MODEL OF TCR SIGNALING TO NF-κB

In the last decade, much progress has been made in defining molecular mechanisms by which the TCR activates the NF-κB transcription factor (72; 75; 77). Most of the key mediators in this cascade are now defined, and many key signal transmission mechanisms have been elucidated. The general consensus understanding is that engagement of the TCR by an MHC-antigen complex initiates downstream CD3 ITAM (immunotyrosine activation motif) phosphorylation by the Src (Sarcoma) family kinases, FYN and LCK (leukocyte C-terminal Src kinase). Phosphorylated CD3 activates the T cell specific tyrosine kinase, ZAP-70 (zeta-chain associated protein kinase), which phosphorylates the adapter proteins LAT (Linker for activation of T cells) and SLP-76 (SH2 domain containing leukocyte protein of 76kDa), causing SLP-76 to bind to VAV1. The VAV1-SLP76-ITK (IL-2 inducible T cell kinase) complex activates PLCγ1 (phospholipase C), generating IP3 (inositol 1,4,5-triphosphate) and DAG (diacylglycerol), which ultimately trigger calcium release and PKC (protein kinase C) activation, respectively. Activation of a specific PKC isoform, PKCθ, connects the above described TCR proximal signaling events to distal events that ultimately lead to NF-κB activation. Importantly, PKCθ activation is also driven by engagement of the T cell costimulatory receptor CD28 by B7 ligands on antigen presenting cells. This molecular interaction activates PI3K (phosphoinositide 3-kinase), inducing recruitment of PDK1 (phosphoinositide dependent kinase) and AKT to the plasma membrane. At the immune synapse (IS), PDK1 phosphorylates and activates PKCθ. PKCθ-mediated phosphorylation of CARMA1 (caspase recruitment domain (CARD)-containing MAGUK protein) triggers a conformational change, causing CARMA1 to bind to BCL10

(B cell leukemia/lymphoma) and MALT1 (mucosa associated lymphoid tissue lymphoma translocation protein), forming the CBM (CARMA1, BCL10, MALT1) complex. Through a mechanism that may involve TRAF6 (TNF receptor-associated factor), both BCL10 and MALT1 become polyubiquitinated. The IKK (IκB kinase) complex is then recruited to the CBM complex via the IKKγ polyubiquitin binding motif. This association leads to polyubiquitination of IKKγ and phosphorylation of IKKβ by TAK1 (TGF-beta activated kinase), activating IKKβ. IKKβ then phosphorylates IκBα, triggering its proteasomal degradation, enabling nuclear translocation of canonical NF-κB heterodimers comprised of p65 (also known as RELA, reticuloendotheliosis viral oncogene homolog A) and p50 proteins. Once in the nucleus, NF-κB governs the transcription of numerous genes involved in T cell survival, proliferation, and effector functions.

RECENT ADVANCEMENTS IN OUR UNDERSTANDING OF THE DISTAL TCR-TO-NF-κB PATHWAY SIGNALING PROTEINS

Deletion of the genes encoding PKCθ and CBM complex proteins results in impaired TCR-induced NF-κB activation. Recent work also identifies a number of additional molecules that regulate this pathway

PKCθ

Phosphorylated PKCθ connects LAT and SLP76 with the CBM complex. The protein kinase PDK1 is considered essential for PKCθ activation as PDK1-deficient Jurkat and primary CD4 T cells show a defect in PKCθ phosphorylation and NF-κB activation (49). However, there is a lack of *in vitro* evidence that PDK1 directly

phosphorylates PKCθ. Moreover, PDK1 activation is dependent on CD28 engagement, while PKCθ IS translocation and NF-κB activation can occur in a purely CD3-dependent manner, without participation of CD28 (3; 49). These observations suggest that another kinase links the TCR-CD3 complex with PKCθ. Indeed, GLK (GCK-like kinase), a SLP76-regulated kinase, was recently reported to directly phosphorylate PKCθ both in vitro and in primary T cells and T cell lines in response to TCR stimulation (7). Additionally, GLK-deficient murine lymph node cells exhibit reduced PKCθ- and IKK-phosphorylation, correlating with reduced cytokine and antibody production. Collectively, these data suggest that PDK1 and GLK1 might function together to induce PKCθ phosphorylation and activate NF-κB. Alternatively, GLK and/or PDK1 may be utilized in an exclusive manner to phosphorylate PKCθ, depending on the activation and/or differentiation state of the T cells, the type of antigen-bearing stimulatory cell, etc.

CARMA1

CARMA1, a critical target of PKCθ phosphorylation, resides in lymphocytes in an inactive state. Extensive CARMA1 mutagenesis data suggest that this inactive state is maintained by intramolecular interactions that prevent the CARMA1 caspase recruitment domain (CARD) from interacting with the CARD of Bcl10. PKCθ phosphorylates human CARMA1 at three serine residues, S552, S645 and S637 (S564, S657, S649 in the mouse) (75). Phosphorylation at S552 and S645 (S564 and S657 in mouse) are critical for the CARMA1 conformational change that enables binding to BCL10-MALT1, leading to further signal transmission. In contrast, S649 phosphorylation suppresses CARMA1-mediated NF-κB and JNK activation (45). It is not known whether S637

(human counterpart of mouse S649) plays a similar role or not. While PKCθ induces CARMA1 S649 phosphorylation in vitro and PKC inhibitors block the phosphorylation event in vivo, there is to date little evidence that PKCθ directly phosphorylates CARMA1 at S649 in living cells. Also, the phosphorylation events of opposing function do not occur simultaneously; the activating phosphorylation at S552/S645 (S564/657 in mouse) is early and transient, whereas the inhibitory phosphorylation at S649 is delayed, but sustained for a longer duration. Considering both the absence of evidence of direct PKCθ phosphorylation of CARMA1 S649 and the rapid PKCθ activation kinetics post-TCR activation, it remains a strong possibility that the delayed CARMA1 S649 phosphorylation is mediated by an unidentified PKCθ-dependent kinase that is activated and/or interacts with CARMA1 in a delayed manner.

BCL10

As a result of the above modifications and interactions of CARMA1, the constitutively associated BCL10-MALT1 complex associates with CARMA1, forming the CBM complex. Immediately following TCR stimulation, BCL10 is phosphorylated and ubiquitinated. BCL10 post-translational modification is complex, with many reported sites of modification(75). The regulation and significance of many modifications remain poorly understood. To date, evidence suggests that IKKβ is one of the principal kinases responsible for BCL10 phosphorylation. Initially, IKKβ-phosphorylation of BCL10 stabilizes the CBM complex, but subsequent IKKβ phosphorylation of BCL10 triggers BCL10 dissociation from MALT1 and/or BCL10 degradation (79). Thus BCL10 phosphorylation may be an important step for terminating TCR signals to NF-κB.

Interestingly, calcineurin, a calcium dependent phosphatase, has been reported to dephosphorylate BCL10, stabilizing the CBM complex and enhancing NF-κB activation.

An area of intense recent investigation involves elucidation of the mechanism and purpose of BCL10 ubiquitination. Reports indicate that BCL10 is modified by K63-polyubiquitination (5; 50) or both K48- and K63-polyubiquitination with K63- preceding K48-polyubiquitination (82). Mutagenesis data suggest that both K48- and K63-polyubiquitin chains are conjugated exclusively to lysines 31 and 63 of Bcl10. The identity of the BCL10 ubiquitin ligase is highly controversial, with NEDD4 (neural precursor cell expressed, developmentally down-regulated) and Itch (60), cIAP2 (cellular inhibitor of apoptosis) (22), βTrCP (beta-transducin repeats-containing protein) (40) and TRAF6 (82) all implicated as E3 ligases targeting BCL10. These uncertainties aside, the emerging consensus is that BCL10 ubiquitination serves two important purposes; initial transmission of the NF-κB activation signal followed by BCL10 degradation and signal termination (40; 50; 60). BCL10 ubiquitination is important for signal transmission, as ubiquitin chains create binding sites for IKKγ (82) and p62 (50) two molecules critical for NF-κB activation.

MALT1

MALT1, the third member of the CBM complex, plays a more nebulous role in TCR activation of NF-κB. Initial studies suggested MALT1 functions as a scaffolding protein that participates in NF-κB activation by connecting the CBM complex with TRAF6. Later studies showed that MALT1 contributes less to TCR activation of NF-κB than BCL10 or PKCθ in primary mouse T cells (32) and that silencing MALT1

expression in Jurkat reduces but does not completely block IκBα phosphorylation (54). Moreover, the protease activity of MALT1 is associated with regulation of diverse cellular functions, most of which are distinct from NF-κB signal transduction. To date, four MALT1 substrates, BCL10, A20, CYLD (cylindromatosis) and RELB (reticuloendotheliosis viral oncogene homolog B), have been identified. MALT1 cleavage of BCL10 and CYLD regulates T cell adhesion (54) and JNK (c-Jun N-terminal kinase) activation (74) respectively, with no detectable effect on NF-κB signal transduction. Another target of MALT1 cleavage is A20, a known inhibitor of NF-κB activation (8) . However, MALT1 cleaves only a small fraction of the total cellular A20 pool and blockade of MALT1 protease activity fails to limit IKK activation. Thus, the significance of A20 cleavage as a mechanism regulating TCR signaling to NF-κB remains uncertain. Among known MALT1 substrates, RELB is most compelling as an NF-κB signal mediator that is cleaved to regulate NF-κB activation. MALT1-dependent RELB cleavage and concomitant degradation leads to increased RELA and c-REL DNA binding (18; 19). How RELB degradation affects RELA or c-REL activity is not well understood, but it might reflect competition between different NF-κB heterodimers for DNA binding sites, or inhibition of canonical activation by gene products of the non-canonical (i.e., RELB-dependent) pathway.

IKK COMPLEX

A key step in TCR activation of NF-κB is CBM complex-dependent K63-polyubiquitination of IKKγ. TRAF6 has been proposed as the ubiquitin ligase that performs this key function. However, TRAF6-deficient T cells do not show impaired NF-

κB activation, suggesting either that TRAF6 does not play such a role, or that there are redundant ubiquitin ligases that compensate for loss of TRAF6. For example, TRAF2, an ubiquitin ligase recruited by the caspase-8-FLIP complex is also capable of polyubiquitinating IKKγ. Another possible candidate is the ubiquitin ligase MIB2 (mind-bomb 2), which binds to BCL10 and promotes IKKγ ubiquitination and NF-κB activation in transfection-overexpression experiments. Thus, it is possible that several ubiquitin ligases contribute to K63-polyubiquitination of IKKγ. Activation of IKK requires a combination of IKKγ ubquitination and IKKβ phosphorylation. The latter process is mediated by the protein kinase TAK1 (TGF-beta activated kinase 1). TAK1 activation seems to be dependent on PKCθ, but not on the CBM complex members CARMA1 and BCL10. However, the precise mechanism of PKCθ-mediated TAK1 activation is not well-defined

The above studies demonstrate that, rather than the early understanding of TCR activation of NF-κB as a simple linear cascade (PKCθ→CBM complex→IKK), there is a complex web of interconnected signaling molecules that link the TCR to NF-κB. In particular, there is accumulating evidence of multiple signaling inputs converging on key proteins, particularly CARMA1 and BCL10. Additionally, the mechanistic understanding of the crucial functions of certain mediators in transmitting the activating signal to NF-κB, e.g., MALT1, is incomplete. Also, the precise roles and relative importance of kinases recently implicated as regulators of this pathway, including PDK1 (phosphoinositide dependent kinase 1), GLK (GCK-like kinase), HPK-1 (hematopoietic progenitor kinase 1), and CK1α (casein kinase 1 alpha) remain to be well-defined. Cross-talk between the TCR-to-NF-κB pathway and other cellular processes, such as regulation

of the actin cytoskeleton and T cell-APC interactions, is an emerging area of interest for which there is currently very limited mechanistic understanding.

NF-κB

Nuclear Factor kappa B consists of a five member family of transcription factors that exist in homo- or hetero-dimers (72; 77). The members are RELA, RELB, cREL, p100/p52 and p105/p50. "NF-κB" is generally used to refer to the RELA-p50 activating heterodimer. In un-stimulated T cells, NF-κB is sequestered in the cytosol by its binding partner IκB. IκB is phosphorylated by IKK, triggering proteasomal degradation, freeing NF-κB to translocate to the nucleus and drive transcription of target genes.

CONCLUSIONS

Recent findings have significantly altered our views of TCR signaling to NF-κB. Certain mediators, such as PKCθ and CARMA1, are phosphorylated by multiple kinases, dispelling early models that postulated a simple linear cascade by which the TCR transmits activating signals to NF-κB. A number of essential post-translational modifications and their downstream effects have now been identified. For example, Bcl10, once thought to be a simple adaptor connecting CARMA1 to MALT1, is now known to undergo K63-polyubiquitination, triggering association with p62 and activation of IKK. Additionally, numerous mechanisms of negative regulation have been recognized, indicating that the TCR-to-NF-κB pathway is tightly modulated. Precise control of NF-κB activation may guarantee production of exact levels of cell cycle proteins, thereby avoiding failed cell division and apoptosis. Despite these recent

advances in our understanding of this pathway, there remain many mechanistic details that are poorly understood.

AUTOPHAGY

Types of autophagy

Autophagy is one of the two major processes by which eukaryotic cells degrade their cellular proteins (38). Autophagy can be categorized into three distinct types: microautophagy, chaperone mediated autophagy (CMA) and macroautophagy (44). Microautophagy involves lysosomal uptake of cytosolic proteins by direct budding through the lysosomal membrane. CMA occurs through LAMP2a (lysosome associated membrane protein) transporter and HSC70 (heat shock cognate 70) chaperone-mediated direct import of cytosolic proteins into lysosomes. In the case of macroautophagy, cytosolic proteins and cellular organelles are taken up by autophagosomes and degraded by lysosomes. As macroautophagy is a major focus of this thesis, it is described in further detail, below.

The process of macroautophagy

The process macroautophagy (henceforth termed autophagy) begins with formation of a membranous structure termed isolation membrane, derived from endoplasmic reticulum, Golgi or plasma membrane (44). The isolation membrane takes up cytosolic contents, and two ends of the isolation membrane unite to form a double lipid bilayered structure, called an autophagosome, thereby trapping the cytosolic contents. Subsequently, the autophagosome fuses with a lysosome, resulting in

degradation of autophagosome contents by lysosomal enzymes. A highly conserved group of proteins called Atg (autophagy-related gene) proteins regulate the process of autophagy. Autophagosome formation is initiated by Atg6/Beclin-1 and class III PI3K (phosphoinositide 3-kinase). Two additional ubiquitin-like systems drive the process of autophagy. The first system involves sequential activation of Atg12 by the ubiquitin-E1 like protein Atg7 and by ubiquitin-E2 like protein Atg10, followed by conjugation of Atg12 to Atg5. Finally, Atg16 binds non-covalently with the Atg5-12 conjugate, resulting in formation of a large Atg5-12/Atg16 protein complex. Atg16 is required for targeting of Atg5-12 to the isolation membrane. The second system involves the processing of protein Atg8/LC3 (light chain 3) by the protease Atg4, resulting in formation of LC3-I. This is followed by sequential activation of LC3-I by Atg7 and Atg3 and subsequent attachment of the LC3 C-terminus to the membrane lipid PE (phosphatidylethanolamine). This last modification results in conversion of cytosolic LC3-I to isolation membrane/autophagosome-bound LC3-II.

Selective and Non-selective autophagy

Autophagy was initially thought to be a mechanism of bulk degradation of random cellular proteins and organelles that allows the cell to recycle its contents and survive under conditions of cell stress and starvation. However, a growing body of evidence suggests that autophagy can also selectively target and degrade protein aggregates, damaged cellular organelles and intracellular pathogens (55). The process of selective autophagy is mediated by sequential target protein polyubiquitination, followed by binding of polyubiquitinated proteins to adapter molecules that traffic the target

proteins to autophagosomes. Several proteins can function as the adapter molecule, such as p62, NBR1, NDP52, and optineurin. These proteins are functionally similar, in that each can bind both to polyubiquitin chains and to autophagosome associated proteins such as LC3, through two different domains. Importantly, emerging data show that selective autophagy of multiple signaling proteins modulates the degree of activation multiple signaling cascades (discussed in details in Chapter 4)

HYPOTHESIS

APC-mediated T cell stimulation leads to rapid recruitment of PKCθ to the cell membrane-associated IS. This membrane-proximal event is closely followed by formation of cytosolic clusters of the signaling molecules, Bcl10 and Malt1, called POLKADOTS, which are vesicular in nature. Additionally, the POLKADOTS were also reported to be the sites where Bcl10-Malt1 adapter proteins communicate with the downstream signaling molecule TRAF6 which signals to NF-κB. Based on the above data, we hypothesize that: *POLKADOTS are cytosolic sites of both transmission of TCR activation signals to the transcription factor NF-κB, and the sites of autophagic degradation of actively signaling Bcl10 molecules, that ultimately lead to termination of NF-κB activation.*

AIMS WITH RATIONALE

1. *Identify the mechanism of Bcl10 degradation and determine the functional importance of Bcl10 degradation in TCR-to-NF-κB signaling*. As TCR

stimulation leads to Bcl10 association with cytosolic vesicles with kinetics similar to the kinetics of Bcl10 degradation, the process of autophagy may be responsible for the degradation process. Determining the mechanism of Bcl10 degradation and its possible effect on the transcription factor NF-κB will help uncover a critical T cell signal regulatory mechanism. This work is described in chapter 2.

2. *Elucidate how Bcl10-Malt1 POLKADOTS help transmit the TCR activation signal generated at cell surface to the cytosolic transcription factor NF-κB*. As presence of POLKADOTS have a high degree of correlation with NF-κB activation, and as Bcl10-Malt1 at POLKADOTS interact with the downstream mediator TRAF6, POLKADOTS may be a crucial signaling intermediate that connects the cell surface TCR to cytosolic NF-κB. Such a finding would represent a significant advance in our understanding of how signals are transmitted from the cell surface to cytosol-resident signaling molecules. In Chapter 3 we perform experiments to evaluate the connection between POLKADOTS and terminal activation of NF-κB.

POTENTIAL CLINICAL RELEVANCE

Effective regulation of TCR-to-NF-κB signaling is central to both initiation of a productive T cell mediated immune response to pathogens and for limiting the degree of T cell activity, as unrestricted and persistent NF-κB activation can lead to autoimmune diseases and neoplasms. Revealing the precise mechanisms of transmission and termination of the TCR activation signal in the cytosol might open up new targets that

can be modulated to control the degree of T cell activity. Specific examples of possible clinical applications and benefits to basic research are discussed in detail in Chapter 4.

CHAPTER 2: Selective autophagy of the adaptor protein Bcl10 modulates T cell receptor activation of NF-κB

Suman Paul[1], Anuj K. Kashyap[1,2], Wei Jia[3], You-Wen He[3], and Brian C. Schaefer[1,2]

[1]Department of Microbiology and Immunology, and [2]Center for Neuroscience and Regenerative Medicine, Uniformed Services University, Bethesda, MD 20814, USA, and [3]Department of Immunology, Duke University Medical Center, Durham, NC 27710, USA.

Published in Immunity, 2012 Jun 29;36(6):947-58

SUMMARY

The adaptor protein Bcl10 is a critically important mediator of T cell receptor (TCR)-to-NF-κB signaling. Bcl10 degradation is a poorly understood biological phenomenon suggested to reduce TCR activation of NF-κB. Here we have shown that TCR engagement triggers the degradation of Bcl10 in primary effector T cells, but not in naïve T cells. TCR engagement promoted K63-polyubiquitination of Bcl10, causing Bcl10 association with the autophagy adaptor, p62. Paradoxically, p62 binding was required for both Bcl10 signaling to NF-κB and gradual degradation of Bcl10 by autophagy. Bcl10 autophagy was highly selective, as it spared Malt1, a direct Bcl10 binding partner. Blockade of Bcl10 autophagy enhanced TCR activation of NF-κB. Together, these data demonstrate that selective autophagy of Bcl10 is a pathway-intrinsic homeostatic mechanism that modulates TCR signaling to NF-κB in effector T cells. This homeostatic process may protect T cells from adverse consequences of unrestrained NF-κB activation, such as cellular senescence.

INTRODUCTION

Antigen stimulation of the T cell receptor (TCR) initiates a complex signaling cascade, culminating in the initiation of a transcriptional program, which drives T cell proliferation and differentiation. The NF-κB transcription factor is a particularly important target of TCR signaling, playing a central role in driving entry into cell cycle via stimulating transcription of numerous effector molecules, including interleukin-2 (IL-2) (71; 78). The adaptor protein, Bcl10, plays a key role in transmitting signals from the TCR to NF-κB. In the absence of Bcl10, T cells are unable to efficiently proliferate and differentiate in response to TCR engagement (57; 61; 76).

Previous studies have suggested that a TCR-dependent mechanism targets Bcl10 for proteolysis, in concert with activation of NF-κB. Although these studies suggested that Bcl10 degradation may be a mechanism to limit TCR signals to NF-κB, the data supporting such a model are limited. Additionally, the molecular mechanism of Bcl10 degradation remains highly controversial, with different groups publishing data supporting diverse degradatory mechanisms (22; 40; 60; 82; 87). Also, almost all experiments in previous studies were performed with long-term tumor cell lines, such as Jurkat. It is therefore unclear to what extent the phenomenon of Bcl10 degradation is relevant to the biology of primary T cells.

Macroautophagy (henceforth termed autophagy) is a cellular process by which cytosolic constituents are engulfed in double-membrane encapsulated vesicles, followed by delivery to lysosomes for degradation. Autophagy can serve as a survival mechanism under conditions of metabolic starvation and growth factor withdrawal, via non-selective degradation of cytosolic constituents for re-use (6; 41). Emerging evidence suggests that

autophagy can also target specific proteins for destruction. Specifically, data suggest that this specialized type of autophagy, referred to as *selective autophagy*, can target specific proteins or organelles for degradation. In general, proteins enter the selective autophagy pathway following post-translational modification with K63-polyubiquitin chains. K63-polyubiquitinated proteins are then bound by p62 (also called SQSTM-1) or by functionally related autophagy adaptor proteins, followed by engulfment in autophagosomes (34; 36; 38).

Interestingly, recent data have shown that TCR stimulation induces autophagy (39), that autophagy contributes to T cell survival and antigen-dependent proliferation (52), and that autophagy-deficient T cells produce more interleukin-2 (IL-2) than their wild-type counterparts (27). These data suggest that TCR-dependent autophagy limits the production of T cell effector molecules such as IL-2 that are essential mediators of T cell proliferative responses. However, the mechanistic link between TCR-induced autophagy and the modulation of T cell effector responses remains to be determined. In this study, we have established that Bcl10 is degraded via selective autophagy, reducing TCR activation of NF-κB and limiting NF-κB-dependent effector responses. This study therefore implicates selective autophagy as a mechanism that modulates antigen receptor signaling and, more generally, as an intrinsic mechanism that can restrain activation of a ligand-initiated signaling cascade.

RESULTS

Bcl10 associates with autophagosomes following TCR stimulation

Our previous microscopy studies demonstrated that TCR signaling leads to oligomerization of Bcl10 and Malt1, forming punctate cytosolic structures called POLKADOTS, which may include a vesicular component (56). To identify vesicular structures associated with POLKADOTS, we used anti-CD3 to activate D10 T cells expressing Bcl10-cyan fluorescent protein (CFP) and MALT1-yellow fluorescent protein (YFP). We also stained these T cells with antibodies directed against a variety of intracellular vesicle markers. Confocal microscopy analysis showed that LC3 and ATG12, markers for autophagosomes, closely co-localized with Bcl10 and MALT1 in POLKADOTS (Fig. 1A). Pearson's co-localization analysis showed higher correlation between Bcl10 and LC3 compared to the other vesicular markers (Fig. 1B). Notably, Lamp2, a lysosomal marker, also showed increased co-localization with POLKADOTS (Fig. 1B).

To confirm that autophagosomes associate with POLKADOTS, we stably expressed a red fluorescent protein (RFP)-LC3 recombinant protein in D10 cells. At 20 min post-activation, D10 T cells showed induction of punctate cytosolic RFP-LC3 signals, representing TCR-induced autophagosomes (39). RFP-LC3^{+} autophagosomes co-localized with cytosolic Bcl10 and MALT1-containing POLKADOTS (Fig. 1C). At 120 min, the Bcl10-CFP signal was lost, reflecting post-activation Bcl-10 degradation (22; 40; 60; 82; 87), and the remaining MALT1-YFP was coalesced into one or several large aggregated structures. Together, these co-localization data suggest that POLKADOTS interact with vesicles of the autophagy-lysosomal degradation system.

Bcl10 degradation occurs in effector T cells, but not in naïve T cells

To assess whether or not Bcl10 degradation occurs in primary T cells, we purified $CD4^+$ and $CD8^+$ T cells from C57BL/6 mice. Cells were stimulated with anti-CD3+anti-CD28 and analyzed by immunoblotting to measure Bcl10. We observed no change in Bcl10 at 0 and 2 hr post-stimulation and increased Bcl10 by 24 hr stimulation (Fig. 1D). To reconcile this lack of Bcl10 degradation in stimulated naïve primary T cells with the clear Bcl10 degradation observed in D10 T cells by our group (Fig. 1C and data not shown) and in the Jurkat T cell line and additional cell types by others (22; 40; 60; 82; 87), we hypothesized that Bcl10 degradation might be a function of T cell differentiation, since D10 is a terminally differentiated Th2 cell clone. To test this hypothesis, we in vitro differentiated $CD4^+$ Th2 effector cells and $CD8^+$ Tcm cells (Fig. S1A, B). These differentiated effectors were then re-stimulated with anti-CD3+anti-CD28, and Bcl10 degradation was assessed via immunoblotting. Both $CD4^+$ Th2 cells and $CD8^+$ Tcm cells showed reduced Bcl10 at 2 hr compared to unstimulated T cells (Fig. 1D). As a second assay to confirm Bcl10 degradation in primary effector cells, we expressed Bcl10-GFP in $CD4^+$ Th2 and $CD8^+$ Tcm cells. Flow cytometry analysis showed reduced median fluorescence of Bcl10-GFP at 2 hr post-anti-CD3+anti-CD28 stimulation in both effector cell types (Fig. 1E, Fig. S1C).

We next examined Bcl10 re-distribution in primary effector T cells. We stimulated $CD4^+$ Th2 cells for 0 min and 20 min, followed by antibody staining and confocal microscopy to visualize endogenous Bcl10. This analysis showed that Bcl10 exhibited a diffuse distribution in the absence of stimulation, whereas Bcl10 formed distinct cytosolic clusters following 20 min of anti-CD3+anti-CD28 stimulation (Fig.

S1D). Therefore, endogenous Bcl10 and Bcl10-GFP show highly similar redistribution patterns in primary T effector cells.

Using $CD4^+$ Th2 and $CD8^+$ Tcm cells infected with a Bcl10-GFP retrovirus, we then performed an anti-CD3+anti-CD28 stimulation time course. Via confocal microscopy analysis, we observed formation of Bcl10-GFP cytosolic clusters at 20 min, followed by substantial Bcl10-GFP degradation at 2 hr (Fig. 1F). Also, Bcl10-GFP clusters co-localized with the autophagosome markers, LC3 and ATG12 (Fig. 1G), consistent with the D10 T cell phenotype (Fig. 1C). Bcl10-GFP co-localization with ATG12 also occurred in response to D10 T cell stimulation by cognate antigen presented by an antigen presenting cell (APC) (Fig. S1E). Finally, autophagosome association with Bcl10 was not associated with induction of apoptosis or other mechanisms of cell death, as there was minimal activation of caspase 3 (Fig. S1F) in stimulated D10 T cells. Moreover, the fraction of stimulation-induced cell death was <5% during the first 2 hr of anti-CD3 stimulation, increasing to only ~7% by 8 hr post-stimulation (Fig. S1G). Together, the data in Fig. 1 demonstrate that effector, but not naïve, T cells degrade Bcl10 in response to TCR stimulation. Additionally, TCR-dependent Bcl10 degradation is temporally correlated with close spatial association between Bcl10 cytosolic clusters (POLKADOTS) and autophagosomes. These data suggest that POLKADOTS may be a site of Bcl10 degradation via autophagy.

TCR stimulation triggers K63-polyubiquitination of Bcl10 and Bcl10-p62 physical association

Although signals for selective autophagy of individual proteins are not yet completely understood, both monoubiquitination and K63-polyubiquitination can target proteins for autophagy, whereas K48-polyubiquitinated proteins are typically degraded by the proteasome (34; 36). A previous study reported that Bcl10 is modified by both K63- and K48-polyubiquitin chains following TCR stimulation (82). To assess whether one or more proteins in POLKADOTS are modified by polyubiquitin, we stained anti-CD3 stimulated D10 T cells with a general antibody against polyubiquitin, as well as with antibodies specific for either K48- or K63-polyubiquitin. Confocal microscopy showed that POLKADOTS contained polyubiquitinated proteins. Furthermore, the K63-polyubiquitin antibody intensely labeled the POLKADOTS, whereas the anti-K48-polyubiquitin staining was primarily confined to the nucleus, demonstrating that proteins within POLKADOTS are primarily modified by K63-polyubiquitin chains (Fig. 2A). To assess whether Bcl10 is directly K63-polyubiquitinated in D10 T cells, we immunoprecipitated Bcl10-GFP (following boiling in SDS), using a GFP antibody. Immunoblotting with both the general polyubiquitin antibody and the K63-polyubiquitin antibody revealed a high molecular weight smear only in anti-CD3 activated D10 cells expressing Bcl10-GFP (Fig. 2B). These data therefore support previous observations that Bcl10 is K63-polyubiquitinated in response to TCR ligation (82).

Selective autophagy of K63-polyubiquitinated proteins is mediated by one of several known autophagy adaptor proteins. Interestingly, p62 is both an autophagy adaptor and a protein implicated in promoting NF-κB activation downstream of various

receptors (46), including the TCR (43). We therefore performed several experiments to assess whether POLKADOTS are sites of interaction between p62 and K63-polyubiquitinated Bcl10. Firstly, we immunoprecipitated Bcl10-GFP from unstimulated and anti-CD3-stimulated D10 T cells. Immunoblotting revealed that while Bcl10-MALT1 association was relatively insensitive to stimulation, the Bcl10-p62 interaction increased following TCR stimulation (Fig. 2C). We next used confocal microscopy to visualize endogenous p62 in D10 T cells expressing Bcl10-CFP, MALT1-YFP, and RFP-LC3. As expected, in unstimulated T cells, p62 showed primarily a punctate distribution (p62 "speckles"), due to the self-aggregation that is induced by the N-terminal PB1 domain (46). Upon anti-TCR stimulation, we observed p62 speckles co-localizing with autophagosomes (RFP-LC3) and Bcl10+Malt1 POLKADOTS (Fig. 2D). We also confirmed these data via expressing YFP-tagged p62 in D10 T cells and observing co-localization of YFP-p62 and Bcl10-CFP POLKADOTS following anti-CD3 stimulation (Fig. S2A). We obtained similar results with $CD4^+$ Th2 cells, in which we observed cytosolic p62 speckles co-localizing with Bcl10-GFP POLKADOTS, following anti-CD3+anti-CD28 stimulation (Fig. 2E). Endogenous Bcl10 also showed similar co-localization with endogenous p62 in $CD4^+$ Th2 cells (Fig. S2B). Additionally, we observed Bcl10-GFP association with p62 in response to antigen+APC stimulation (Fig. S2C). Finally, antibody staining data showed that endogenous NBR1, another autophagy adaptor which can oligomerize with p62 (33), also colocalized with Bcl10-GFP POLKADOTS (Fig. S2D).

Previous studies have suggested that p62 interacts with Malt1 and that Malt1 can be K63-polyubiquitinated in TCR-dependent manner (11; 43). Thus, published data

suggest that polyubiquitination of either Bcl10 or Malt1 (or both proteins) could account for the intense K63-polyubiquitin labeling of POLKADOTS and the association with p62. However, the fact that Bcl10, but not Malt1, was rapidly degraded following TCR activation suggested that only Bcl10 enters the autophagy pathway. Therefore, to ascertain if Bcl10, and not MALT1, interacts with autophagosomes, we immunoprecipitated LC3 from lysates of D10 T cells, using an RFP antibody. As expected, p62 co-immunoprecipitated with RFP-LC3 in lysates from both stimulated and unstimulated T cells, showing that p62 constitutively binds LC3 (Fig. 2F). In contrast, Bcl10 co-immunoprecipitated with RFP-LC3 only after anti-CD3 stimulation. These data suggest that a TCR-dependent process, such as K63-polyubiquitination of Bcl10, is required to promote Bcl10 interaction with p62 and LC3. Importantly, we failed to detect MALT1 in the RFP-LC3 immunoprecipitates, consistent with the observation that there is no appreciable degradation of Malt1 in response to TCR engagement. Because Bcl10 and Malt1 are constitutively associated within T cells (76) (see also Fig. 2C), and there was no detectable Malt1 in complexes containing LC3, p62, and Bcl10 (Fig. 2F), our data suggest that a highly selective mechanism targets Bcl10 for association with autophagosomes. Together, the data in Fig. 2 suggest that, in response to TCR signaling, Bcl10 is K63-polyubiquitinated and physically associates with p62 speckles and $LC3^+$ autophagosomes.

Expression of p62 is required for TCR-dependent Bcl10 degradation

To assess whether p62 plays a role in Bcl10 degradation, D10 cell lines expressing Bcl10-GFP were infected with either the empty shRNA vector or a p62-

shRNA (p62-silenced) (Fig. 3A). We stimulated these cell lines with anti-CD3 (0 hr and 2 hr) and quantified Bcl10-GFP via flow-cytometry. While control cells showed a substantial decrease in Bcl10-GFP fluorescence in response to anti-CD3 stimulation, Bcl10-GFP fluorescence remained unchanged in the p62-silenced cells (Fig. 3B). We then performed confocal microscopy experiments to assess NF-κB activation, by identifying cells with RelA nuclear translocation. In the absence of stimulation, control and p62-silenced cells showed diffuse Bcl10 and cytosolic RelA, as expected. Following 20 min of anti-CD3 stimulation, Bcl10 formed POLKADOTS in control cells, while remaining diffusely localized in p62-silenced cells. Also, RelA translocated to the nucleus in control cells, whereas it remained cytosolic in p62-silenced cells. At 120 min, control cells had greatly reduced Bcl10 fluorescence, reflecting Bcl10 degradation, whereas Bcl10 fluorescence remained unchanged in p62-silenced cells, consistent with flow cytometry data. Also, we continued to observe RelA in the nucleus in control cells, whereas RelA remained cytosolic in the p62-silenced cell line (Fig. 3C). Quantification of data in the Fig. 3C experiment revealed a significant decrease in both cells forming Bcl10 POLKADOTS and cells with nuclear RelA in the p62-silenced line. Moreover, those p62-silenced cells that formed Bcl10 POLKADOTS were the same cells that exhibited RelA nuclear translocation (Fig. 3D-E and data not shown). Staining with anti-p62 revealed that the small percentage of p62-silenced cells with Bcl10 POLKADOTS retained detectable amounts of p62 that co-localized with POLKADOTS (Fig. S3A).

To exclude the possibility that the observed phenotypes in the p62-silenced cell line were due to an unrecognized general defect in TCR signal transduction, we assessed phosphorylation of the kinases ERK1 and ERK2, which are activated via a TCR-

dependent mechanism that is distinct from the NF-κB cascade (72). Although TCR-dependent Bcl10 degradation occurred in control cells and not in p62-silenced cells, similar ERK1 and ERK2 phosphorylation was observed in both cell lines (Fig. S3B). Finally, we assessed whether p62 acts upstream or downstream of the IκB kinase complex (IKK), which initiates terminal NF-κB activation via promoting degradation of IκBα. We stimulated D10 T cells or a D10 p62-silenced cell line with anti-CD3 and measured phosphorylation of IKKα+IKKβ and degradation of endogenous Bcl10 by immunoblotting. Whereas unmanipulated D10 T cells exhibited both Bcl10 degradation and robust phosphorylation of the IKK complex in response to anti-CD3, there was little to no IKK phosphorylation or Bcl10 degradation in p62-silenced cells (Fig. S3C). Thus, consistent with previous data (43), this experiment shows that p62 acts upstream of IKK in the TCR-to-NF-κB pathway. Taken together, the data in Figs. 3 and S3 show that expression of p62 in T cells is necessary for both TCR-dependent activation of NF-κB and TCR-directed degradation of Bcl10.

Polyubiquitination of Bcl10 is required for Bcl10 degradation

A recent study using Jurkat cells has established that polyubiquitination of human Bcl10 occurs at lysines 31 and 63 (82). Furthermore, blockade of Bcl10 polyubiquitination by mutation of these residues to arginines dramatically inhibits TCR mediated NF-κB activation and Bcl10 degradation (82). To confirm these data, we expressed GFP-tagged wild-type and K31R,K63R (KK.RR) Bcl10 in the D10 Th2 T cell clone. Cells were stimulated for 0 or 20 min with anti-CD3, followed by immunoprecipitation of Bcl10-GFP. Immunoblotting revealed K63-polyubiquitination of

wild-type Bcl10 and greatly reduced polyubiquitination of the Bcl10-KK.RR mutant (Fig. 4A). The KK.RR mutant was also deficient in NF-κB activation (as assessed by degradation of IκBα), consistent with previous observations (82).

Confocal microscopy analyses revealed that whereas T cells expressing wild-type Bcl10-GFP formed POLKADOTS at 20 min and exhibited substantial loss of Bcl10-GFP fluorescence by 120 min, the KK.RR mutant showed no TCR-dependent change in distribution or fluorescence. Examination of the ERK pathway in both cell lines showed equivalent anti-CD3-induced phosphorylation of both ERK1 and ERK2, confirming intact TCR signaling in both cell lines (Fig. S4). Confocal microscopy analysis showed that wild-type Bcl10 co-localized with p62 clusters at 20 min post-stimulation, while the KK.RR mutant failed to translocate to p62 clusters (Fig. 4C). The data in Fig. 4A-C collectively suggest that K63-polyubiquitination of Bcl10 is essential for the Bcl10-p62 interaction and Bcl10 degradation.

To directly establish a requirement for Bcl10 polyubiquitination for association between p62 and autophagosomes, we immunoprecipitated wild-type and KK.RR Bcl10-GFP, assessing the association of each form of Bcl10 with p62 and the autophagosome membrane proteins, LC3 and Atg5-12. Immunoblotting showed that wild-type Bcl10 associated with p62, LC3, and Atg5-12 in response to anti-CD3 stimulation. However, the polyubiquitination-deficient Bcl10-KK.RR mutant failed to associate with both p62 and autophagosomes in response to stimulation (Fig. 4D, E). Together, the data in Fig. 4 suggest that modification of Bcl10 by K63-polyubiquitination mediates Bcl10 association with p62 and autophagosomes.

TCR-dependent autophagy is a mechanism of Bcl10 degradation

To specifically assess the effect of the autophagy-lysosomal degradation pathway on Bcl10 degradation, we employed three pharmacological agents that block this pathway at differing points and by distinct mechanisms: 3-methyladenine (3-MA), a type III PI3-kinase inhibitor that suppresses autophagosome formation (63); Bafilomycin A1 (BafA1), which blocks the H^+ATPase pump, thereby preventing acidification of lysosomes and/or lysosome-autophagosome fusion (35); and E64d, an inhibitor of lysosomal proteases (80). Following pretreatment of cells with inhibitors, we used flow cytometry to quantify Bcl10-GFP at 0 hr and 2 hr post anti-CD3 stimulation. There was no effect of inhibitors on Bcl10-GFP in the absence of stimulation. Following anti-CD3 stimulation, control cells pre-treated with vehicle exhibited a clear decrease in Bcl10-GFP median fluorescence intensity (MFI), reflecting degradation of Bcl10-GFP, while all three drug treatments inhibited Bcl10 degradation (Fig. 5A). The partial effect of all three drugs on Bcl10 proteolysis suggested that the proteasome may also contribute to Bcl10 degradation. Indeed, p62 can direct ubiquitinated proteins to both the autophagy-lysosome pathway and the proteasome (47; 64). To assess the potential role of the proteasomal pathway on Bcl10 degradation, we pre-treated D10 T cells with the proteasomal inhibitor MG132, followed by 0 hr or 2 hr anti-CD3 stimulation. Flow-cytometry analysis revealed a partial block of Bcl10 degradation, similar to the effects of autophagy inhibitors (Fig. 5B). Analogous effects on Bcl10 degradation were observed when the same inhibitors were used with C57BL/6 Th2 cells expressing Bcl10-GFP (Fig. 5C).

To confirm the specificity of the chemical inhibitors of autophagy, we employed a genetic approach. Specifically, we in vitro differentiated Th2 cells from mice in which the essential autophagy gene, *Atg3*, can be conditionally inactivated (25). *Atg3* deletion was induced in Th2 cells via 4-hydroxytamoxifen (4-OHT) treatment. Following 2 hr stimulation with anti-CD3+anti-CD28, we compared the degree of Bcl10 degradation between WT control ($Atg3^{f/f}$) and *Atg3*-deleted ($Atg3^{f/f}$ ER-Cre) cells, in the presence and absence of MG132 (Fig. 5D). Whereas control cells ($Atg3^{f/f}$) exhibited robust degradation of endogenous Bcl10, much less Bcl10 degradation occurred in Th2 cells lacking ATG3. Moreover, while MG132 treatment partially blocked Bcl10 degradation in the $Atg3^{f/f}$ control cells, the residual Bcl10 degradation in cells lacking ATG3 was completely or nearly completely blocked by MG132 treatment. These data provide strong genetic evidence that TCR-mediated degradation of endogenous Bcl10 is controlled by autophagy, with a contribution from the proteasomal system.

TCR-dependent autophagy is responsible for separating Bcl10 from Malt1

To assess the effect of autophagy inhibitors on the subcellular distribution of Bcl10, we pretreated D10 T cells expressing Bcl10-CFP, MALT1-YFP and RFP-LC3 with 3-MA or BafA1. We then stimulated cells with anti-CD3 for 20 min or 2 hr, followed by confocal microscopy analysis. Consistent with data in Figs. 1-2, untreated controls exhibited co-localization between Bcl10- and Malt1-containing POLKADOTS and LC3 puncta at 20 min post-stimulation (Fig. 5E). By 120 min post-stimulation, control cells showed depletion of Bcl10-GFP, and concentration of the remaining Malt1 in large aggregates. Cells treated with BafA1 exhibited a phenotype indistinguishable

from controls at 20 min. However, at 120 min, Bcl10 remained closely associated with $LC3^+$ puncta in BafA1-treated cells. Importantly, most of the cellular Malt1 no longer co-localized with the Bcl10 puncta, forming aggregates within the cell that were clearly distinct from the $Bcl10^+LC3^+$ aggregates. In the case of 3-MA treatment, we observed normal formation of Bcl10- and Malt1-containing POLKADOTS at 20 min, but very weak formation of $LC3^+$ autophagosomes, consistent with expectations. At 120 min, there was little evidence of Bcl10 degradation, and Bcl10 remained tightly associated with the large Malt1 aggregate.

Combined with the data of Figs. 1-4, the data in Fig. 5E suggest a sequential process by which Bcl10 becomes associated with p62, captured by $LC3^+$ autophagosomes, and degraded via the autophagy-lysosome pathway: TCR stimulation leads to K63-polyubiquitination of Bcl10. Via the ubiquitin-binding (UBA) domain of p62, Bcl10 becomes concentrated at p62 speckles, and the resulting p62-Bcl10 clusters efficiently promote signal transduction to IKK. Simultaneously, via interaction with the LC3 interaction region (LIR) of p62, autophagosomes assemble at p62 speckles, engulfing K63-polyubiquitinated Bcl10, modulating signals from Bcl10 to IKK. Bcl10 is then degraded within autophagosomes (with contributions by the proteasome), leaving aggregates of Malt1 that coalesce over time.

The autophagy of Bcl10 was mechanistically associated with the physical separation of Bcl10 and Malt1, as demonstrated by the existence of spatially distinct $Bcl10^+LC3^+$ puncta and larger aggregates containing Malt1 (and not Bcl10), following to BafA1 treatment. In other words, in both untreated and BafA1-treated cells, autophagosomes engulf Bcl10, without capturing Malt1. BafA1 treatment inhibits a later

degradative step, blocking autophagosome-lysosome fusion and/or lysosomal acidification, thereby leaving Bcl10 enclosed within $LC3^+$ vesicles at 120 min. By contrast, when autophagosome formation is blocked by 3-MA, Bcl10 is not captured from the p62 speckles by autophagosomes. Thus, in the absence of autophagosome formation, Bcl10 and Malt1 are never physically separated, remaining co-localized during the coalescence of Malt1 aggregates. Overall, the data in Fig. 5E suggest that autophagy is an essential component of the mechanism that separates Bcl10 from Malt1, enabling the selective TCR-dependent degradation of Bcl10.

Inhibition of autophagy enhances TCR mediated NF-κB activation

A prediction of the above model is that 3-MA treatment or *Atg3* deletion should leave a signaling-competent form of Bcl10 associated with Malt1 and p62 at late time points following TCR engagement. In contrast, BafA1 and E64d treatment should not block the autophagy of Bcl10, but rather its later degradation by the lysosome. Consequently, the Bcl10 that becomes engulfed within autophagosomes in BafA1 and E64d-treated cells should be unable to signal to NF-κB because it is not accessible to downstream cytoplasmic signaling partners. Thus, 3-MA treatment and *Atg3* deletion should enhance signaling to NF-κB, whereas BafA1 and E64d treatment should have no impact on signaling to NF-κB. We tested these predictions in several independent assays. First, we generated a D10 cell line expressing both Bcl10-GFP and a Gaussia luciferase reporter gene under control of an NF-κB-dependent promoter. After drug pre-treatment, we stimulated this cell line using anti-CD3. Prior to anti-CD3 stimulation, there was generally no effect of the inhibitors, although we noted a modest increase in basal NF-κB

activity following treatment with the autophagy inhibitor, 3-MA. Following 6 hr of anti-CD3 stimulation, 3-MA pre-treated cells exhibited significantly increased NF-κB activity (approximately 3-fold greater than control). In contrast, lysosomal inhibitors did not significantly impact NF-κB activity in anti-CD3-treated cells (Fig. 6A).

As a second approach, we pre-treated in vitro differentiated Th2 cells with 3-MA, BafA1, E64d, and MG132. Cells were treated for 0 hr or 6 hr with anti-CD3+anti-CD28 and assessed by flow cytometry for expression of CD25, a gene highly dependent on NF-κB activation and Bcl10 expression (1; 32; 57). While 3-MA pre-treated cells showed a significantly higher increase in anti-CD3-induced CD25 expression compared to control cells, the increase in CD25 expression following BafA1 and E64d pre-treatment was indistinguishable from controls (Fig. 6B). MG132, in addition to inhibiting Bcl10 degradation, also prevents proteasomal degradation of IkBa, thereby inhibiting the terminal step leading to NF-κB activation (48). As expected, there was no upregulation of CD25 in MG132 pre-treated cells (Fig. 6B). As a third approach, we measured IL-2 secretion from $CD8^+$ Tcm cells. Following pre-treatment with the same inhibitors employed in Fig. 6B, $CD8^+$ Tcm cells were stimulated with anti-CD3+anti-CD28 for 0 hr or 6 hr, and the amount of IL-2 (also highly NF-κB and Bcl10 dependent (21; 32; 57)) was measured in cell supernatants. Similar to the results of Fig. 6B, treatment with the lysosomal degradation inhibitors, BafA1 and E64d, had little impact on IL-2 secretion, whereas inhibition of NF-κB activation by MG132 treatment prevented IL-2 secretion. Only inhibition of autophagy by 3-MA led to increased IL-2 production in response to anti-CD3 stimulation (Fig. 6C).

To confirm that the 3-MA data truly reflect inhibition of autophagy and not an off-target effect of this drug, we also tested the effect of *Atg3* deletion on anti-CD3+anti-CD28 induction of CD25 expression by Th2 cells as well as the production of IL-2 by Tcm cells (Fig 6D-E). These data confirmed that cells lacking ATG3 ($Atg3^{f/f}$ ER-Cre) showed higher expression of CD25 and greater production of IL-2 than WT control cells ($Atg3^{f/f}$). Taken together, the data in Fig. 6 show that TCR signaling to NF-κB is augmented by inhibition of the autophagy-lysosomal degradation pathway prior to autophagosome formation. Inhibition of later steps (autophagosome-lysosome fusion and lysosomal proteolytic activity) has no impact on NF-κB signaling. These data are therefore consistent with the predictions described above.

DISCUSSION

In this study, we have shown that selective autophagy is a major mechanism of TCR-dependent degradation of Bcl10. Our data are consistent with our previous fluorescence resonance energy transfer (FRET) study, showing a time-dependent dissociation of Bcl10 and Malt1 specifically within the POLKADOTS structures (56). Indeed, Malt1, a constitutive binding partner of Bcl10, is not destroyed in this autophagy process, but remains in aggregates which coalesce over time into a much larger structure (56). Previous data suggest that Bcl10 phosphorylation plays a role in dissociating Bcl10-Malt1 complexes (79). However, even if Bcl10 phosphorylation has a profound effect on the avidity of the Bcl10-Malt1 interaction, it is unclear how Malt1 avoids engulfment by autophagosomes while remaining localized at a site that cannot be distinguished (by conventional confocal microscopy) from the site of autophagosome engulfment of Bcl10.

How, then, is Bcl10 selectively targeted for autophagy, when both proteins are clearly in close proximity to p62 during the capture of Bcl10 by autophagosomes? This complex mechanistic question will require much future work.

Importantly, we found that p62 is crucial both for Bcl10-dependent NF-κB activation and for termination of Bcl10 signaling, via promoting Bcl10 autophagy. As our previous FRET data indicated that Bcl10 signaling partners are enriched at POLKADOTS (56), K63-polyubiquitination of Bcl10 may promote association with and activation of downstream signaling partners by creating Bcl10 clusters that serve as cytosolic signaling platforms. Via the p62-LC3 association, autophagy depleted K63-polyubiquitinated Bcl10 from these signaling platforms, reducing activating signals to NF-κB. It will be important to determine how the formation of Bcl10 signaling complexes and the termination of signaling by Bcl10 autophagy are orchestrated to yield the observed kinetics of NF-κB activation and deactivation downstream of TCR engagement (30).

Additionally, we found that Bcl10 degradation is confined to effector T cells. This observation may reflect the fact that naïve T cells, in contrast to effector T cells, require an extended period of TCR signaling to successfully proliferate (23). Thus, the observed increase in Bcl10 expression in naïve T cells may be necessary for these cells to achieve the precise amount of NF-κB activation required for successful completion of G_1. Conversely, in effector T cells, the degradation of Bcl10 may be necessary to temporally limit stimulation to the time period during which NF-κB signals promote T cell activation and cell cycle entry. This homeostatic mechanism may furthermore protect effector T

cells from undesired consequences of inappropriate activation of NF-κB in later phases of the cell cycle, such as induction of senescence (89) or apoptosis (23).

A growing body of data implicates selective autophagy in diverse cellular processes such as degradation of toxic protein aggregates and processing antigens for presentation to T cells (34; 36; 38). However, we are aware of only one previous study of higher eukaryotes that has identified a role of selective autophagy in directly regulating a signal transduction pathway, as part of normal cellular physiology. A recent publication suggests that selective autophagy of *disheveled* (Dvl) negatively regulates the Wnt pathway (16). Multiple aspects of this regulatory mechanism are strikingly similar to the NF-κB regulatory pathway we have described. For example, the autophagy of Dvl is facilitated by p62, and binding to p62 requires Dvl ubiquitination. Additionally, degradation of Dvl is partially sensitive to MG132, indicating that the proteasome can participate in degradation of ubiquitinated Dvl.

There is also a notable difference between the autophagy-dependent destruction of Dvl and Bcl10. Specifically, data suggest that the destruction of Dvl is initiated by cell stressors, such as starvation, and is therefore not triggered as an integral process within the Wnt pathway. By contrast, in the case of TCR-to-NF-κB signaling, our data indicate that antigen signaling through the TCR triggers both activation of NF-κB and the selective autophagy of Bcl10, inhibiting NF-κB activation. In other words, these findings strongly suggest that Bcl10 autophagy is an integrated homeostatic mechanism allowing the TCR to very precisely control the magnitude and/or kinetics of NF-κB activation in effector T cells. The existence of such a regulatory mechanism is consistent with our recent observation that the TCR-to- NF-κB cascade is digital, with the amount of NF-κB

activation in individual T cells being remarkably invariant, regardless of the intensity of TCR signals (30). In general terms, our data demonstrate that selective autophagy can serve as a built-in homeostatic mechanism by which a receptor precisely controls the extent of activation of a target transcription factor.

Overall, our data establish a molecular mechanism whereby signaling to NF-κB is negatively modulated by TCR-induced autophagy of Bcl10. Our data suggest that Bcl10 degradation is mediated by p62-dependent selective targeting of K63-polyubiquitinated Bcl10 for entry into the autophagy-lysosomal proteolysis system. Combined with the recent report of regulation of the Wnt pathway by a similar selective autophagy process, our data suggest that selective autophagy may be a common mechanism for modulation of diverse signaling pathways. Indeed, while this manuscript was in revision, a report was published describing an autophagy mechanism that limits inflammasome activation in macrophages by a very similar p62- and polybiquitin-mediated process (68).

EXPERIMENTAL PROCEDURES

Cell lines and reagents.

D10 T cells were maintained as previously described (56). Pre-treatments with inhibitors were as follows: 3-methyladenine (MP Biomedicals) in distilled water (1mM),16 hr; Bafilomycin A1 (Enzo Life Sciences) in DMSO (100nM), 1 hr; E64d (Cayman chemicals) in DMSO (10μg/ml), 16 hr; MG132 in DMSO (20μM), 1 hr. Antibodies are detailed in Supplemental Methods.

$CD8^+$ Tcm and $CD4^+$ Th2 cell differentiation.

Lymph nodes and spleens were collected from C57BL/6, *Atg3*$^{f/f}$, or *Atg3*$^{f/f}$ ER-Cre mice (25). Negative bead sorting of $CD4^+$ and $CD8^+$ T cells, $CD8^+$ Tcm cell differentiation, and $CD4^+$ Th2 cell differentiation were performed as described (14; 32; 42). Deletion of *Atg3* via 4-OHT treatment was as described (25). All mouse experiments were approved by the Uniformed Services University Institutional Animal Care and Use Committee.

Flow-cytometry for detection of Bcl10-GFP degradation.

D10 T cells or $CD4^+$ Th2 cells or $CD8^+$ Tcm cells (5×10^5) expressing Bcl10-GFP were stimulated with plate bound anti-CD3 (D10) or anti-CD3+anti-CD28 (primary T cells), pelleted by centrifugation, and fixed using 3% formaldehyde. Flow cytometry was performed using BD LSRII flow-cytometer, as described (32). Data were analyzed using Flowjo software (TreeStar).

Confocal Microscopy and Pearson's co-localization analysis.

Fixation and staining of T cells was as previously described (56). Confocal images were obtained using a 40× 1.4 NA oil objective, a Zeiss 710 NLO microscope, and Zen software. LSM files were exported to Adobe Photoshop for cropping and adjusting contrast levels. POLKADOTS were scored through visual observation of Bcl10 clusters. Nuclear RelA was scored with visual observation of RelA signal overlapping with nuclear DRAQ5 signal. Quantification of co-localization was performed using the Intensity Correlation Analysis plugin in MBF ImageJ (www.macbiophotonics.ca/imagej).

30 cells in each group were analyzed to generate the Pearson's correlation coefficient with a range of +1 (perfect correlation) to -1 (perfect exclusion).

Immunoprecipitation and Immunoblotting.

D10 T cells were stimulated as described (56). Cells were incubated on ice for 30 min in a lysis buffer (83) with 1× Halt protease inhibitor cocktail (Pierce Biotechnology) and 5 mM N-ethylmaleimide. Pre-cleared lysates were incubated with anti-GFP (MP Biomedicals) or anti-RFP (Rockland) overnight at 4ºC. Antibody-antigen complexes were then captured using protein G sepharose beads (GE). Bcl10 ubiquitination was detected as described (82). Briefly, after cell lysis, 1%SDS was added to the lysates and heated for 5 min at 95º C. Lysates were diluted to a concentration of 0.1% SDS, followed by overnight immunoprecipitation with anti-GFP. Immunoblotting was performed as described (56).

Gaussia Luciferase and XTT assays.

For NF-κB luciferase assays, supernatants from 5×10^5 cells/condition were collected at 6 hr post-stimulation and Luciferase activity was measured using a Gaussia Luciferase kit (Targeting Systems). For IL-2 assays, supernatants from 5×10^5 cells/condition were collected at 6 hr post-stimulation and added to 96-well plates loaded with 5000 HT-2 cells/well. HT-2 cells were grown for 48 hr, followed by addition of XTT to measure viability (Biotium). Absorbance (OD) was measured using a spectrometer at 490 nm. Measured OD was converted to ng/ml IL-2 by linear regression, employing a standard curve and Graph Pad Prism 4.0.

Statistical analysis.

For Fig. 3, p-values were calculated using an unpaired two-tailed t-test. For Fig. 6A-C, and E, p-values for the difference in mean between controls and treated cells were calculated by one-way ANOVA with Dunnett's Multiple comparison post-test.

Antibodies.

Primary antibodies used in this study included rabbit anti-Bcl10 (Santa Cruz sc-372), mouse anti-Bcl10 (Santa Cruz Biotechnology sc-5273), rabbit anti-p62 (Sigma P0067200UL), mouse anti-NBR1 (Santa Cruz Biotechnology sc-130380), rabbit anti-MALT1 (SantaCruz Biotechnology sc-28246), mouse anti-GAPDH (Santa Cruz Biotechnology sc-32233), rabbit mouse anti-tubulin (Santa Cruz Biotechnology sc-5286), anti-phosphoERK1 and 2 (Cell Signaling Technology 4370S), rabbit anti-phospho-IKKα/β (Cell Signaling Technology 2694) rabbit anti-caspase-3 (Cell Signaling Technology 9662, gift from R. Panganiban), rabbit anticleaved caspase-3 (Cell Signaling Technology 9661) rabbit anti-LC3 (Novus Biologicals NB100-2220), mouse anti-LC3 (MBL M152-3), rabbit anti-ATG12 (Cell Signaling Technology 2011S),rabbit anti-ATG3 (Sigma A3231), mouse anti-polyubiquitin (Enzo LifeSciences BML-PW8810),rabbit anti-K48 polyubiquitin (Milipore 05-1307), rabbit anti-K63 polyubiquitin (Milipore 05-1308),rabbit anti-RelA (Santa Cruz Biotechnology sc-372), anti-EEA1 (Cell Signaling Technology2411S), anti-Rab4 (BD 610888), anti-Rab5 (BD 610281), anti-Rab11 (Cell Signaling Technology3539S), and anti-Lamp2 (Biolegend 108502). DRAQ5 (Cell Signaling Technology 4084) was used to mark the nucleus. For Western blots, horseradish peroxidase–coupled goat anti-mouse or anti-rabbit secondary antibodies (Jackson ImmunoResearch) were used. For microscopy, secondary antibodies included anti-mouse Alexa488, anti-rabbit

Alexa555, and anti-rabbit Alexa647 (Molecular Probes A21121, A21429 and A21245, respectively). Flow cytometry antibodies included anti-CD4-APC-Cy7 (BD 552051), anti-CD8-APC-Cy7 (BD 557654), anti-IFN -PerCP-Cy5.5 (eBioscience 45-7311-82), anti-IL4-PE (BD 554389), anti-CD62L-PE (BD 553151), anti-CD44-V450 (BD 560541), and anti-CD25-PE (BD 553866).

Cloning, Retroviral constructs and shRNA.

The D10 T cell line co-expressing Bcl10-CFP and MALT1-YFP has been described (Rossman et al., 2006). LC3 was PCR amplified from murine cDNA, tagged with RFP (tdTomato), and cloned into the pEZeo retroviral vector (Schaefer et al.,2001). p62 was cloned from a murine cDNA, fused at the N-terminus to YFP (Citrine), and cloned into the pENeo retroviral vector (Schaefer et al., 2001). Retroviral infection of T cells was as described (Rossman et al., 2006). For expression of Bcl10-GFP in CD8 Tcm cells and CD4 Th2 cells, cells were infected with an MSCV-Bcl10-GFP retroviral vector. To prepare D10 T cells with an integrated NF- B-luciferase reporter, T cells were infected with a self-inactivating MMLV retrovirus containing five multimerized NF- B binding sites and a minimal promoter, cloned upstream of the *Gaussia* luciferase reporter. This cell line was then super-infected with a retrovirus encoding Bcl10-GFP. The Bcl10-KK.RR-GFP construct was created by site-directed mutagenesis of wild-type Bcl10-GFP, introducing the mutations K31R,K63R (Wu and Ashwell, 2008)in murine Bcl10. This mutant was stably introduced into D10 T cells using retroviral transduction with pEhyg (Schaefer et al., 2001). The p62 shRNA (5'-CGCTGACAATGGCTATGTCCTA-3') was cloned into the miR30 cassette of the custom produced vector, MSCV-miR-Neo, which contains a miR-

30 expression cassette upstream of a G418-resistance cassette, which is driven by a phosphogylcerate kinase (PGK) promoter.

Apoptosis assay.

D10 Bcl10-GFP cells were treated with 1 M Staurosporine (gift from Andrew Snow) or stimulated with plate bound 100 g/ml anti-CD3 antibody up to indicated time points, followed by staining with 7AAD (BD 51-68981E) and annexin V (BD 550474) and flow cytometric analysis.

CHAPTER 3: A cytosolic p62-Bcl10-Malt1 signalosome is required for T cell receptor activation of NF-κB in effector T cells

Suman Paul[1] and Brian C Schaefer[1,2,*]

[1]Department of Microbiology and Immunology, and [2]Center for Neuroscience and Regenerative Medicine, Uniformed Services University, Bethesda, MD 20814, USA.

*Corresponding author: Schaefer, B.C. (Brian.Schaefer@usuhs.edu)

(Manuscript for submission in the *Journal of Experimental Medicine* as a Brief Definitive Report)

ABSTRACT

Antigen mediated stimulation of the T cell receptor (TCR) triggers activation of transcription factors, including NF-κB, that are crucial for T cell activation, proliferation and gain of effector function. The terminal events in the TCR-to-NF-κB pathway involve activation of the IKK protein kinase complex, effecting phosphorylation and degradation of IκBα and activation of NF-κB. In this study we demonstrate that activation of IKK occurs in cytosolic p62-Bcl10-Malt1 clusters in effector T cells. Additionally, we observed transient recruitment of phosphorylated IκBα and NF-κB to the cytosolic aggregates prior to nuclear migration of NF-κB. We also show that pharmacological inhibitors block IKK activity in the cytosolic clusters and limit the degree of NF-κB activation. Our findings provide direct evidence that the cytosolic p62-Bcl10-Malt1 signalosome is an essential intermediate in TCR activation of NF-κB.

INTRODUCTION

T cells, upon recognition of antigen-MHC complexes on APCs by cell surface T cell receptors (TCR), initiate a signaling cascade that activates NF-κB, a transcription factor regulating T cell proliferation and differentiation (75). Shortly after TCR engagement, several TCR proximal events lead to activation of the protein kinase, PKCθ. PKCθ mediated Carma1 phosphorylation causes Carma1 to binding to Bcl10 and Malt1, forming the "CBM" complex. An ubiquitin ligase, possibly TRAF6, K63-polyubiquitinates Bcl10 and Malt1, and this modification recruit the IKK complex to Bcl10 and Malt1. IKK activation requires both K63-polyubiquitination of IKKY and phosphorylation of IKKβ, with evidence suggesting the later process is mediated by TAK1. Activated IKK phosphorylates the NF-κB inhibitor, IκBα, triggering its polyubiquitination and degradation. This terminal activation event frees NF-κB to translocate to the nucleus where it activates gene transcription. While biochemical studies in various T cell populations have uncovered the above described TCR to NF-κB signaling sequence in considerable detail, the subcellar mechanisms organizing and regulating these events remain poorly understood.

TCR signaling is initiated at multiple sites on the T cell surface called microclusters (10). Microclusters fuse to form the Immunological Synapse (IS), a structure that develops at the APC and T cell interface. As PKCθ and CARMA1 are recruited to the IS, the IS might provide a stable platform for continuous signaling to downstream mediators (ref). But multiple studies have demonstrated that a stable IS is not required for T cell activation (13; 53). At low antigen density, IS formation is

transient, but the signaling strength is still sufficient to induce CD8 T cell cytotoxicity (53). Experiments in a three dimensional collagen matrix showed that T cells attach with and detach from APCs at a rapid rate (17), which might result in formation of multiple short lived IS. Surprisingly, T cells in which the IS has been interrupted multiple times shows no difference in IFN-γ production compared to T cells with a stable IS (13). Collectively, these studies suggest the existence of a site distinct from the IS, that is capable of maintaining the signaling cascade despite IS disruptions.

In activated T cells, PKCθ and Carma1 are located on lipid rafts (15) along with some fraction of Bcl10, Malt1 and IKK (2; 62). It is therefore unclear how these cell surface signaling molecules communicate with phosphorylated/active form of IKK and the IκBα-NF-κB complex, that are present only in the cytosol (62). Using biochemical analysis, one group reported that post-TCR stimulation, there is formation of an early CBM complex, that matures to a late Bcl10-Malt1 complex, and the later complex inducibly interacts with IκBα (5). Imaging studies from our lab have previously identified presence of cytosolic Bcl10-Malt1 clusters, called POLKADOTS, in D10 T cells and effector T cells (50; 56; 59). The POLKADOTS are capable of communicating with the downstream mediator TRAF6 (56), and presence of these signaling clusters is highly correlated with nuclear NF-κB translocation (29), suggesting a role of POLKADOTS in activating NF-κB. The Bcl10-Malt1 clusters form around the adapter protein p62/SQSTM-1, which constitutively forms cytosolic aggregates called "speckles." p62 knockdown blocks both POLKADOTS formation and NF-κB activation (50). These data are in agreement with observations from another group that reported that

p62 is important for IKK activation in T cells, including CD4+ Th2 cells (43). Thus, in this study, we sought to determine if the Bcl10-Malt1 cytosolic clusters forming around p62 can be the missing connection between the membrane bound PKCθ-CBM complex and the cytosolic IκBα-NF-κB complex. We found that post-TCR stimulation, p62-Bcl10-Malt1 clusters form at locations that are distinct from membrane associated PKCθ and Carma1. Additionally, these cytosolic aggregates provide stable scaffolds for recruitment and phosphorylation of IKK and IκBα that ultimately lead to NF-κB activation.

RESULTS AND DISCUSSION

Cytosolic Bcl10-p62 clusters/signalosomes are sites of IKK and IκBα phosphorylation in effector T cells.

Using primary effector T cells and T cell clones (D10 T cells, which are mouse CD4 Th2 clones), we have previously demonstrated that shortly after stimulation with conalbumin (Ag)-loaded CH12 B cells (APCs) or anti-CD3, the cytosolic Bcl10 and Malt1 proteins form aggregates (POLKADOTS) around cytosolic "speckles" of the adaptor protein p62 (50; 56). To ascertain the subcellular location of key mediators in the TCR-to-NF-κB pathway with respect to the cytosolic Bcl10 clusters, we stimulated D10 cells with Ag-loaded APC. We then used confocal microscopy to image PKCθ-CFP, Bcl10-YFP, and endogenous Carma1 and p62. We observed that at 10 and 20 min post-stimulation, PKCθ and Carma1 translocated to the IS (Figure 7A). While we detected some Bcl10 at the IS, co-localizing with PKCθ, the majority of Bcl10 existed as cytosolic aggregates that co-localize with p62 (Figure 7A, C). Post T cell stimulation, FRET analysis have demonstrated that Bcl10 is physically associated with TRAF6, an ubiquitin ligase involved in recruiting and ubiquitinating IKK (75), in the cytosolic Bcl10-Malt1

clusters (56). As others have shown that phosphorylated IKK is detected solely in cytosol (62), we hypothesized that the active forms of IKK exist in association with cytosolic Bcl10-Malt1 POLKADOTS. Staining with a phospho-specific antibody that binds the active forms of IKKα/β revealed no/little signal in unstimulated cells (Figure 7B) (with minor non-specific cell membrane staining). 20 min post-stimulation, we observed phospho-IKK co-localizing with the cytosolic Bcl10 clusters, and not with the IS. Similar results were obtained with D10 T cells stimulated with anti-CD3 coated coverslips (Figure 7D). In the penultimate step of NF-κB activation, activated IKK phosphorylates IκBα, causing proteasome mediated phospho-IκBα degradation, allowing NF-κB nuclear translocation. Due to the rapid degradation kinetics of phospho-IκBα, it is abundant only for a short period of time post-T cell activation. Accordingly, at 10 min post-stimulation, we detected phosphorylated IκBα co-localizing with Bcl10, Malt1 and phospho-IKK (Figure 7D). The phospho-IκBα signal was lost by 20 min post-stimulation, presumably due to the rapid proteasomal degradation of IκBα.

Collectively, our data suggest that TCR stimulation leads to recruitment of PKCθ and Carma1 to the IS. Bcl10 transiently interacts with CARMA1 at the IS, but subsequently forms Bcl10-Malt1 clusters/POLKADOTS around cytosolic p62 aggregates. Both activated IKK and phosphorylated IκBα co-localize with p62-Bcl10-Malt1 aggregates, suggesting that these structures initiate the terminal steps in NFκB activation.

RelA transiently co-localizes with cytosolic Bcl10 signalosomes before translocating to the nucleus.

In unstimulated T cells, NF-κB resides in the cytosol bound to IκBα. IκBα degradation unmasks a nuclear localization signal, allowing NF-κB to enter the nucleus, where it promotes transcription of target genes. The NF-κB family consists of five proteins that exist as homo or heterodimers (77), with RelA(p65)-p50 being the most common heterodimer. As we successfully detected presence of phospho-IκBα along with Bcl10-Malt1 clusters, we hypothesized that RelA should also be present in the aggregates with IκBα. Imaging revealed a cytosolic RelA distribution before T cell stimulation (Figure 8A-B). At 10 min post-stimulation, both with antigen loaded APCs and anti-CD3 coated coverslips, we observed RelA co-localizing with cytosolic Bcl10-Malt1 aggregates, but not yet translocated to the nucleus. By 20 min post-stimulation, RelA was no longer associated with the POLKADOTS aggregates and it was highly enriched in the nucleus, demonstrating that IκBα degradation and NF-κB activation occur between 10 and 20 min post-TCR stimulation. Taken together, these observations support our hypothesis that p62-Bcl10-Malt1 clusters are the intracellular sites where the terminal steps in the TCR-to-NF-κB pathway take place.

Pharmacological inhibitors block IKK phosphorylation at cytosolic Bcl10 signalosomes, causing reduced RelA activation.

To further confirm that the IKK phosphorylation observed at POLKADOTS/p62-Bcl10-Malt1 clusters is responsible for RelA activation, we utilized two different pharmacological inhibitors to block phosphorylation process; BAY 11-7082 (31), an IKK kinase domain inhibitor, and 5Z-7-oxozeaenol, a specific inhibitor of TAK1 (66), the kinase responsible for IKK phosphorylation in the TCR-to-NF-κB pathway. Following

anti-CD3 stimulation, inhibitor treated D10 T cells showed reduced IKKα/β phosphorylation without altering TCR-dependent ERK1/2 phosphorylation (Figure 9A), which demonstrates the specific action of the inhibitors on the TCR-to-NF-κB pathway. Confocal microscopy revealed that while inhibitor treatment did not affect PKCθ IS translocation and Bcl10 cluster formation (Figure 9B), there was a striking loss of phospho-IKK from Bcl10 clusters in both BAY 11-7082 and 5Z-7-oxozeaenol treated cells, compared to control/DMSO treated cells (Figure 9B). Next we looked at the effect of BAY 11-7082 and 5Z-7-oxozeaenol on RelA nuclear translocation. Stimulation with antigen loaded APCs or anti-CD3 coated coverslips, showed a reduction in the degree nuclear RelA staining (Figure 9C, D), without any alteration in PKCθ IS translocation (Figure 9C) or Bcl10 cluster formation (Figure 9C, D). Quantifying the ratio of nuclear to cytosolic RelA yielded a statistically significant decrease in nuclear RelA intensity with inhibitor treatment in both antigen-loaded APCs and anti-CD3 stimulation groups compared to control cells (Figure 9E). Altogether, these observations show that inhibition of IKK phosphorylation prevents staining of Bcl10 POLKADOTS with the anti-phospho-IKK, demonstrating the specificity of the phospho-IKK antibody in this assay. Furthermore, these data demonstrate that phosphorylation of IKK and activation of RelA are downstream of PKCθ IS translocation and Bcl10 POLKADOTS formation.

Collectively, our data demonstrate that T cell stimulation leads to rapid IS recruitment of PKCθ and Carma1. This is followed by an early transient association of Bcl10 with the IS, followed by robust and persistent association of Bcl10 with p62 speckles. These aggregates, which we refer to as the POLKADOTS signalosome, are a

site of enrichment of the phosphorylated IKK complex, suggesting that IKK is activated at these structures. We also observed that the cytosolic p62-Bcl10-Malt1 clusters are transiently associated with phosphorylated IκBα and cytosolic RelA, followed by persistent nuclear RelA translocation. As expected, co-localization of phospho-IKK with Bcl10 clusters and nuclear translocation of RelA were inhibited by blocking activating phosphorylation of IKK. Together, these data strongly suggest that the cytosolic POLKADOTS signalosome, rather than the plasma membrane IS, is the site of terminal activation of the IKK complex in effector T cells.

MATERIALS AND METHODS

Cell Lines, reagents and antibodies.

The CD4+ Th2 clone D10 and CH12 B cells (APC) were maintained in Click's (EHAA) media containing 10% FBS, with and without IL-2 respectively as described in (59). The fluorescent tagged PKCθ, Bcl10 or Malt1 genes were cloned into pE retroviral constructs, that were used to generate retrovirus and infect D10 T cells to produce the following cell lines: D10 PKCθ-CFP Bcl10-YFP, described in (59) or D10 Bcl10-CFP+Malt1-YFP, described in (56). For APC mediated stimulation, CH12 B cells (APCs) were loaded with 125 μg/ml conalbumin (cognate antigen for D10) (Sigma) overnight in 37°C incubator, followed by mixing and centrifugation with equal number of D10 T cells to initiate T cell-APC conjugate formation. The D10 T cell and CH12 B cell conjugates were placed on coverslips and fixed at indicated time points. For anti-CD3 stimulation, plates or coverslips were coated with 100 μg/ml anti-CD3 antibody overnight at 4°C, washed 6X with PBS the next day, and D10 T cells were placed on top of coated surface, up to indicated time points. Pretreatment with inhibitors were as follows: BAY

11-7082 (Calbiochem) in DMSO (5 μg/ml) was added to cells 5 min post-stimulation, 5Z-7-oxozeaenol (Enzo) in DMSO (2 μM) was added 30 min before stimulation. In both conditions, cells were stimulated for 20 min. Primary antibodies used in this study included rabbit anti-CARMA1 (Enzo ALX-210-903), rabbit anti-p62 (Sigma P0067200UL), mouse anti-tubulin (Santa Cruz Biotechnology sc-5286), anti-phospho ERK1 and 2 (Cell Signaling Technology 4370S), rabbit anti-phospho-IKKα/β (Cell Signaling Technology 2694), mouse anti-phospho-IκBα (Cell Signaling Technology 9246), rabbit anti-RelA (Santa Cruz Biotechnology sc-372). DRAQ5 (Cell Signaling Technology 4084) was used to mark the nucleus. Secondary antibodies for microscopy included anti-rabbit or anti-mouse IgG1 Alexa555, and anti-rabbit or anti-mouse IgG1 Alexa647 (Molecular Probes). Western blot secondary antibodies included Horseradish peroxidase–coupled goat anti-mouse or anti-rabbit secondary antibodies (Jackson ImmunoResearch).

Confocal Microscopy.

Cells were fixed with 3% paraformaldehyde for 10 min, washed 3x with PBS, permeabilized with 0.2% Triton X-100, 0.1% azide in PBS for 5 min, washed 3x with PBS, blocked with 10% FBS in tissue culture media (DMEM) for 20 min, and incubated with primary antibody (diluted in blocking media) overnight. The next day, cells were washed 6x with PBS, stained with secondary antibody (diluted in blocking media), washed 6x with PBS and mounted in glycerol phosphate-buffered saline with the photobleaching inhibitor, p-phenylenediamine. For nuclear stains, cells were incubated with DRAQ5 (1:1000 dilution in PBS) for 5 min, after the secondary antibody stain. Confocal images were obtained with 40X 1.4 NA oil objective, a Zeiss 710 NLO

microscope, and Zen software. LSM image files were exported to Adobe Photoshop for adjusting contrast levels and cropping. ImageJ software was used to quantify nuclear and cytosolic fluorescence levels. Values were plotted on Graph Pad Prism 4 software to generate graphs and p-values calculated by unpaired two-tailed t test (Figure 3E).

Immunoblotting.

Cells were lysed in 1x Laemmli buffer, followed by sonication and boiling for 5 min. Lysates were separated by SDS-PAGE gel electrophoresis, transferred to nitrocellulose membrane, blocked with 5% milk, or 3% BSA (for phospho-specific antibodies), and probed with indicated primary antibodies (diluted in blocking media) overnight at 4°C. The next day, the membrane was washed and probed with species-specific HRP-conjugated secondary antibodies (diluted in blocking media) for 1 hr at ambient temperature. Images were developed with Fuji LAS-3000 CCD camera system.

ACKNOWLEDGEMENTS

Supported by grants from US National Institutes of Health (Al057481 to BCS), Center for Neuroscience and Regenerative Medicine (CNRM) (to BCS), and pre-doctoral fellowships (to SP) from the American Heart Association (10PRE3150039) and the Henry M Jackson Foundation. The views expressed are those of the authors and do not necessarily reflect those of the Uniformed Services University or the Department of Defense. The authors declare no competing financial interests.

CHAPTER 4: Discussion

REVIEW OF CHAPTER 2 RESULTS

Parts of this section have been published in *Autophagy, 2012 Nov 1;8(11):1690-2* titled as: "Selective autophagy regulates T cell activation"

Suman Paul[1] and Brian C Schaefer[1,2,*]

[1]Department of Microbiology and Immunology, and [2]Center for Neuroscience and Regenerative Medicine, Uniformed Services University, Bethesda, MD 20814

[*]correspondence to B.C.S. (brian.schaefer@usuhs.edu)

As described in Chapter 2, our findings reveal new details regarding the mechanism of Bcl10 signaling and regulation of Bcl10 activity in the TCR-to-NF-κB pathway. Specifically, we demonstrate that TCR-dependent Bcl10 K63-polyubiquitination triggers interaction with p62 speckles (cytosolic p62 clusters). We also show that the Bcl10-p62 interaction is crucial for TCR signaling to IKK and consequent activation of NF-κB. The p62 speckles simultaneously interact with $LC3^+$ autophagosomes. The p62-LC3 interaction results in autophagic uptake and degradation of p62-bound Bcl10, thereby depleting the active polyubiquitinated form of Bcl10 and limiting the magnitude of NF-κB activation. Thus, p62 is paradoxically required both for Bcl10 activation of NF-κB and for limiting activation of NF-κB via directing autophagy of Bcl10. This is consistent with observations from another group that showed the importance of p62 in NF-κB signaling in effector CD4 Th2 cells (43). Additionally, later studies from our lab revealed that the p62-Bcl10-Malt1 clusters are the sites of IKK and

IκBα phosphorylation (discussed in Chapter 3), two important steps in the TCR-to-NF-κB activation pathway. The p62-Bcl10 interaction is most likely mediated by Bcl10 K63-polyubiquitin chains binding to the C-terminal UBA (ubiquitin associated) domain of p62. Recruitment of $LC3^+$ autophagosomes to sites of Bcl10-p62 clusters presumably depends on the p62 LC3 interacting region (LIR) binding to the N-terminal region of LC3.

Remarkably, autophagic Bcl10 degradation is highly selective, resulting in degradation of only Bcl10, but not its direct binding partner, Malt1, which is also present in POLKADOTS. This observation is consistent with a previous study from our lab that showed a time dependent decrease in the Bcl10-Malt1 interaction within the POLKADOTS (56). Biochemical analysis revealed that LC3 interacts with only Bcl10, and not Malt1. Moreover, unlike Bcl10, Malt1 is not degraded after T cell activation. Therefore, Bcl10 is targeted for autophagy in a highly selective manner. Our data suggest that an intact autophagy mechanism is required for the physical separation of Malt1 from Bcl10. Notably, Bcl10 and Malt1 clusters form at locations that cannot be distinguished from sites of autophagic punctum formation by conventional light microscopy. Thus, elucidating the mechanism of selective Bcl10 uptake by autophagosomes will require a more detailed understanding of the dynamic molecular interactions occurring at p62 speckles following TCR stimulation. Such studies may be aided by electron microscopy or super-resolution microscopy, to assess whether Bcl10 and MALT1 become segregated into distinct p62-proximal sub-domains.

It is possible that TCR stimulation activates autophagy, as one study reported that IKK is capable of inducing autophagy in several different mammalian cell lines (9). Thus, in one model, the TCR activation signal can pass through Bcl10 and activate IKK leading the induction of autophagy. The newly formed autophagosomes can seek out and degrade the actively signaling Bcl10 molecules; thereby completing a negative feedback loop that controls degree of TCR mediated NF-κB activation (Figure10). A second method of autophagy activation might depend on an undiscovered pathway that directly links the TCR to the autophagy machinery, without involvement of IKK.

We observed that Bcl10 degradation was profoundly inhibited by p62 silencing or by blocking Bcl10 K63-polyubiquitination. In contrast, pharmacological or genetic inhibition of autophagy only partially inhibited Bcl10 degradation. Experiments with the proteasome inhibitor MG132 revealed that proteasomes also play a significant role in Bcl10 degradation. As p62 is known to interact with proteasomes (64), the simplest interpretation of these data is that p62 directs K63-polyubiquitinated Bcl10 to autophagosomes and proteasomes (Figure 11). Alternatively, a parallel pathway of TCR-dependent K48-polyubiquitination of Bcl10 might target some Bcl10 for proteasomal degradation. One study has reported that Bcl10 is both K63 and K48-polyubiquitinated, with K63 modification preceding K48 (81). It is therefore also possible that an ubiquitin editing enzyme (such as A20 or CYLD) clips off the K63-polyubitin chains and replaces them with K48 chains, allowing Bcl10 to be channeled towards proteasomes (Figure11). The precise cellular location of Bcl10 K63-poluibiquitination is not known. Bcl10 K63-polyubiquitnation likely occurs before Bcl10 forms POLKADOTS, as Bc10

polyubiquitination seems to be a requirement for Bcl10 aggregate formation. Through imaging studies, we have detected minor amounts of Bcl10 transiently present at the IS shortly after TCR stimulation (see chapter 3). Thus, Bcl10 may become polyubiquitinated at the IS, and the modified Bcl10 might subsequently attach to p62 clusters through the UBA domain on p62.

A number of TCR-to-NF-κB distal signaling mediators undergo K63-polyubiquitination, including Bcl10, Malt1 and IKKγ. But as discussed in the Chapter 1 introduction section, each modification has a different purpose and fate. Initially, the Bcl10 and Malt1 K63-polyubiquitin chain allows for IKKγ recruitment to Bcl10-Malt1, and the transmission of the activation signal. Subsequently K63-polyubiquitinated Bcl10 is degraded by autophagosomes, while K63-polyubiquitinated Malt1 is spared. One study indicates that post-TCR stimulation, Malt1 K63-polyubiquitin chains are cleaved off by the ubiquitin editing enzyme A20 (12), which might limit the amount Malt1 interaction with p62 and later uptake by autophagosomes. It is however currently not known whether the K63-polyubiquitinated IKKγ is targeted by autophagosomes for degradation or not.

An emerging body of evidence suggests that selective autophagic degradation of signaling proteins might serve as a common mechanism for regulation of several different signaling pathways. Autophagic degradation of TRIF and TRAF6, Dishevelled protein, and inflammasomes, suppress TLR signaling (24), Wnt activation (16), and IL-1β production (69), respectively. It is likely that future studies will reveal additional examples of selective autophagy regulating activation of diverse signaling pathways.

The abovementioned studies conducted on the TLR (24) and Wnt (16) pathway, also uncovered a role of proteasomes in the destruction of the target proteins, which is similar to our observation regarding TCR dependent Bc10 proteolysis. Collectively, these reports indicate that p62 and other autophagy adapters are connected to both the proteasomal and autophagic degradation mechanisms. Why both proteasomes and autophagosomes are both devoted towards destruction of certain cellular signaling proteins is not well understood. However, it is known that unrestricted and persistent activation of certain transcription factors, such as NF-κB, can lead to development of autoimmune diseases and neoplasms (28), cellular senescence (88), or apoptosis (37). It is therefore possible that the cell utilizes two overlapping protein destruction mechanisms to ensure that proper cellular function continues even when one the degradation pathways is blocked or inhibited.

REVIEW OF CHAPTER 3 RESULTS

As described in Chapter 2, we demonstrate that TCR stimulation causes rapid PKCθ and Carma1 translocation to the IS. Bcl10 transiently associates with PKCθ and Carma1 at the IS, and subsequently co-localizes with cytosolic p62, resulting in formation of aggregates termed POLKADOTS. This observation is supported by biochemical evidence from another group that showed that Bcl10-Malt1 dissociates from the early CBM complex to form cytosolic structures that interact with IκBα (5). Additionally, we observed that IKK phosphorylation occurs at the p62-Bcl10-Malt1 clusters in the cytosol and not at the cell surface IS. This is in agreement with a previous FRET study from our lab which showed cytosolic Bcl10 at the POLKADOTS interacts

with TRAF6, an ubiquitin ligase known to be responsible for IKK recruitment and activation by polyubiquitination. As IKK phosphorylation is critical for IκBα degradation and RelA nuclear translocation, it is highly likely that p62 is required for RelA/NF-κB activation. Our hypothesis of the requirement of p62 clusters for RelA activation is supported by two observations; 1. p62 shRNA silencing blocks RelA translocation (as discussed in Chapter 2); and 2. There is failure to sustain IKK phosphorylation in T cells derived from p62 knockout mice (43). Future imaging studies performed in p62 deficient T cells will further enhance our understanding of the precise role of p62 in recruiting the IKK complex.

Using confocal microscopy and an antibody specific for phosphorylated IKKα/β, we detected the presence of phospho-IKK in the cytosolic p62-Bcl10-Malt1 aggregates/POLKADOTS. Biochemical evidence also suggests that phospho-IKK exists only in the cytosol (62), which supports our imaging analysis. However, the unphosphorylated/inactive IKK exists both in the cytosol and cell surface lipid rafts (2; 62). Furthermore, the precise cellular location of TAK1, the kinase responsible for directly phosphorylating IKK, is also unclear. Imaging experiments with cells stained with a TAK1 antibody, or cells expressing fluorescent tagged TAK1 protein will help in establishing the simultaneous localization of the positions of TAK1 and IKK. This will reveal the cellular location of IKK-TAK1 interaction that leads to IKK phosphorylation and also suggest how phospho-IKK is recruited to cytosolic POLKADOTS.

The study of mediators downstream of IKK revealed that cytosolic p62-Bcl10-Malt1 clusters transiently associate with phosphorylated IκBα and cytosolic RelA. This is followed by loss of the phosphorylated IκBα signal and migration of cytosolic RelA to the nucleus. The last two events indicate successful IκBα degradation that permits RelA nuclear translocation. Thus cytosolic POLKADOTS seem to be the site of both initial RelA/NF-κB activation (by phosphorylation and degradation of IκB), and later termination of RelA/NF-κB activation (by degradation of Bcl10). Such coupling of signaling activation and termination at the same location is also seen at the immunological synapse (10). Initially, TCR clustering at the cell surface leads to the generation of the activation signal. Later, at the c-SMAC (central supramolecular activation cluster), the TCR is internalized into endosomes and degraded, which limits the amount of activation signal. Therefore the critical sites of cellular signal transmission also appear to serve as checkpoints in the signaling pathway in order to regulate and fine-tune the amount of activation signal.

Curiously, POLKADOTS are not the only cytosolic protein clusters capable of activating NF-κB. Post-viral infection, viral RNA present in cell cytoplasm triggers a signaling cascade which activates NF-κB and induces cellular interferon secretion. The cytosolic protein RIG-I (retinoic acid inducible gene) detects the presence of viral RNA and subsequently binds to the mitochondrial outer membrane protein MAVS (mitochondrial antiviral signaling protein) through a CARD-CARD interaction. This results in formation of large MAVS aggregates on mitochondrial surface, that are extremely efficient at activating IKK and NF-κB in the cytosol (20). Thus, it is possible

that the final steps in NF-κB activation occurs on distinct cytosolic signaling protein aggregates that form in response to upstream signals in multiple different cell types, and not only in T cells.

Overall our study indicates that the terminal steps in the TCR-to-NF-κB pathway are played out in the cytosol. We have thus provided a crucial missing connection concerning how a signal originating at the cell surface is transmitted to a cytosolic transcription factor.

RESEARCH RELEVANCE

While studying the formation and function of POLKADOTS, we uncovered two significant events in TCR-to-NF-κB signal transduction. First, POLKADOTS provide a scaffold for interaction and activation of the terminal mediators in NF-κB pathway. Second, the critical signaling protein Bcl10 present in POLKADOTS is degraded by a mechanism that requires p62, autophagosomes and proteasomes, resulting in termination of the NF-κB activation signal. Thus by intervening in the process of formation and dissolution of POLKADOTS, it might be possible to control the level of NF-κB activation and thus alter T cell behavior. Below we discuss some specific strategies that can be utilized to achieve such a therapeutic goal.

Possible clinical applications

Perhaps the most obvious target for intervention will be the adapter protein p62, as p62 is required for optimum T cell NF-κB activation. Additionally, as p62 is required only for effector T cell function, modifying p62 will limit only the activation of effector

cells, while having little to no effect on activation of the naïve cell population. Thus p62 targeting might have the added advantage of not interfering with antigen triggering of naïve T cells, in contrast to existing immunosuppressive drugs which are broadly inhibitory for T cell activation. However, devising a method that blocks p62 might be difficult. Because p62 is an adapter molecule, with no enzymatic function, small peptide inhibitors that can be designed to block molecules with enzymatic functions will not have an effect on p62. Silencing p62 expression using the RNAi pathway will certainly work in reducing cellular p62 levels and having the desired effect. But major disadvantage to this approach will the method of delivery of sufficient amounts of siRNA into primary cells which is proving to be quite challenging (67).

A second target of intervention will be the process of autophagy itself. Pharmacological agents capable of inducing or blocking autophagy should theoretically be able to inhibit or activate NF-κB, thereby modifying T cell function both directions. Rapamycin (also known as sirolimus) is a well known immunosuppressive drug that blocks T cell function and is used extensively to prevent transplanted organ rejection (58). Rapamycin exerts its actions by binding to and inhibiting the activity of the protein mTOR (mammalian target of rapamycin). As signaling through mTOR is required for proper activity of cyclins and several protein kinases essential for T cell progression through cell cycle, by blocking mTOR, rapamycin inhibits T cell proliferation. The above described process is the accepted mechanism of action of Rapamycin. But rapamycin has a long documented role as one of the most potent inducers of autophagy. As mTOR has the additional function of inhibiting autophagosome formation, rapamycin-mediated blockade of mTOR function also activates autophagy. So it is tempting to speculate that

rapamycin might be limiting T cell function by the following additional mechanism: rapamycin blocks mTOR which activates autophagy, and, in turn, autophagy degrades the signaling protein Bcl10, which results in reduced NF-κB and T cell activity. Thus our study might have uncovered a previously unknown mechanism by which the clinically proven drug rapamycin blocks T cell activation. Along this line, we should conduct studies to examine whether the newly developed autophagy inducing peptides have a possible immunosuppressive effect (70). However, both autophagy inducers and p62 blockers will reduce function of all effector T cell populations, and will share a major limitation of our existing immunosuppressive drugs, which is broad and non-specific reduction of T cell function, which exposes recipients to opportunistic infections.

Several therapies are attempting to utilize autologous T cells, expanded in vitro and modified to recognize tumor cells, to induce remission or perhaps even to cure neoplasms (84). In these therapies, often the amount of available T cells becomes a severe limiting factor. In Chapter 2 we reported that autophagosome formation inhibition by 3-MA greatly increased NF-κB activation, IL-2 secretion and IL-2 receptor expression. As IL-2 and signaling through IL-2 receptor is required for T cell progress through cell cycle, this observation seems to suggest that 3-MA treated T cells might demonstrate a more rapid antigen induced proliferation. If future studies show that post 3-MA treatment, T cells expand to a greater degree than untreated T cells, this method can be harnessed to generate a greater number of T cells in-vitro from a small parent population in short period of time. However, unrestricted NF-κB activation also has certain well-documented deleterious outcomes, such as senescence and apoptosis (51).

Thus the viability of the expanded T cell population has to be carefully analyzed before their practical applications.

Certain individuals or families with hypo- or hyper-responsive immune cells harbor activating or blocking mutations in the TCR-to-NF-κB signaling proteins that can be revealed by sequencing and comparison to reference genomes (73). We uncovered a role of the autophagy adapter protein p62 and the process of autophagy, in both initially activating and subsequently limiting the degree of T cell function. As mentioned in Chapter 1, the autophagy process is coordinated by a family of highly conserved Atg proteins. Variations in p62 and Atg protein expression or function due to small changes in the DNA sequences (for example single nucleotide polymorphisms) can render certain individuals more or less capable of carrying out the process of selective autophagy, and by extension better or worse at modulating T cell function. Thus comparing the Atg and p62 sequence, (in addition to the sequences of known TCR-to-NF-κB signaling proteins) might explain the possible mechanism of altered T cell behavior.

A word of caution

The observations described in Chapters 2 and 3 were based on in-vitro studies performed by utilizing a protein over-expression system in mouse D10 T cell clones and confirmed by using endogenous proteins in mouse primary effector T cells. So far, we are aware of only one report that showed presence of cytosolic MALT1 POLKADOTS in a human T cell line (Jurkat cells) (4). Furthermore, recently it has been shown that mouse immune responses to sepsis, trauma and burn, have limited correlations with the human immune responses (65). Thus before we try to seek out human applications of this study, experiments with human naïve and effector cells, preferably differentiated in-vivo, should

be undertaken to validate the presence of similar T cell signaling mechanisms that we observed in mouse T cells.

Possible basic science applications

Even if the therapeutic and diagnostic methods outlined above do not bear fruit, the discovery of a fundamental mechanism of cellular signal transduction regulation has other potential benefits.

Lessons learned by elucidating a basic process in biology enable us to predict and then look for the presence of similar mechanisms in related systems. Our study showed significant differences in mechanism of TCR-to-NF-κB signaling between naïve and effector T cells. In response to antigen stimulation, effector cells utilize p62 and form POLKADOTS for rapid signaling to NF-κB. In contrast, naïve cells with low p62 expression and little or no POLKADOTS formation activate NF-κB at a much slower pace. This is consistent with other observations of T cell behavior, as activation of naïve cells occurs in the order of hours to days, compared to effector cells that take only minutes to hours. Thus, if the differences in naïve and effector cell behavior are at least partially due to differences in signaling protein expression and the mechanism of signal transduction, it is possible that some of the differences seen between different effector T cell populations (T_H1 vs. T_H2 vs. T_{reg} etc) are also due to alterations in cellular signal transduction. Indeed a recent report suggested that differential behavior of PKCθ alters the function of T_{reg} cells compared to other effector T cells (85; 86). It is therefore likely that over time, numerous additional modifications of signal transduction, each specific for a particular T cell population will emerge. Ultimately, the general TCR-to-NF-κB pathway that we know now may be replaced by multiple population-specific TCR-to-NF-κB pathways. Understanding those individual variations in signaling between different T

cell types will lead to development of therapies that target those variations and produce more specific alterations in our immune response.

Comprehending the underlying processes behind an elementary phenomenon allows us to tie together multiple seemingly unrelated observations, and put forward a unified theory that attempts to explain the unconnected reports. Researchers study T cells from multiple different angles. Over the last decade, various groups published observations that initially appeared to have little or no connection with each other. First, studies investigating crosstalk between autophagy and T cell behavior reported two unexplained phenomenon: T cell stimulation activates autophagy and autophagy-deficient T cells produce greater amounts of IL-2 compared to their wild type counterparts (26; 27). Second, several T cell signaling researchers were observing the association of Bcl10 with lysosomes or cytosolic vesicles, but the precise mechanism and effect of this observation remained unclear (4; 56; 60). Lastly, a group performing biochemical analysis on the adapter protein Bcl10 reported that Bcl10 K63-polyubiquitination blockage not only inhibited TCR signal transduction, but also stopped the process of TCR-dependent Bcl10 degradation (82). Our observations demonstrated how K63-polyubiquitinated Bcl10 is selectively taken up by autophagosomes and degraded by lysosomes which results in reduced T cell IL-2 secretion. By elucidating a fundamental principal of signaling regulation, this study helped explain the mechanistic process underlying the disparate observations.

CONCLUSION AND THESIS SUMMARY

The observations discussed in this thesis have expanded our understanding of the mechanisms of both signal transmission and termination from the TCR to NF-κB. We demonstrate that TCR stimulation leads to rapid translocation of PKCθ and Carma1to the cell surface IS, followed by Bcl10-Malt1 clustering around cytosolic p62 aggregates, named POLKADOTS. These cytosolic clusters act as scaffolds for the recruitment and phosphorylation of IKK and IκBα, which ultimately lead to RelA nuclear translocation. Additionally, we show that the K63-polyubiquitinated Bcl10 at the POLKADOTS are selectively taken up and degraded by autophagolysosomes. The loss of actively signaling Bcl10 molecules results in decreased signaling to RelA and reduced T cell activation. Thus our study has uncovered two previously unknown processes that regulate TCR-mediated NF-κB activation in effector T cells.

FIGURES

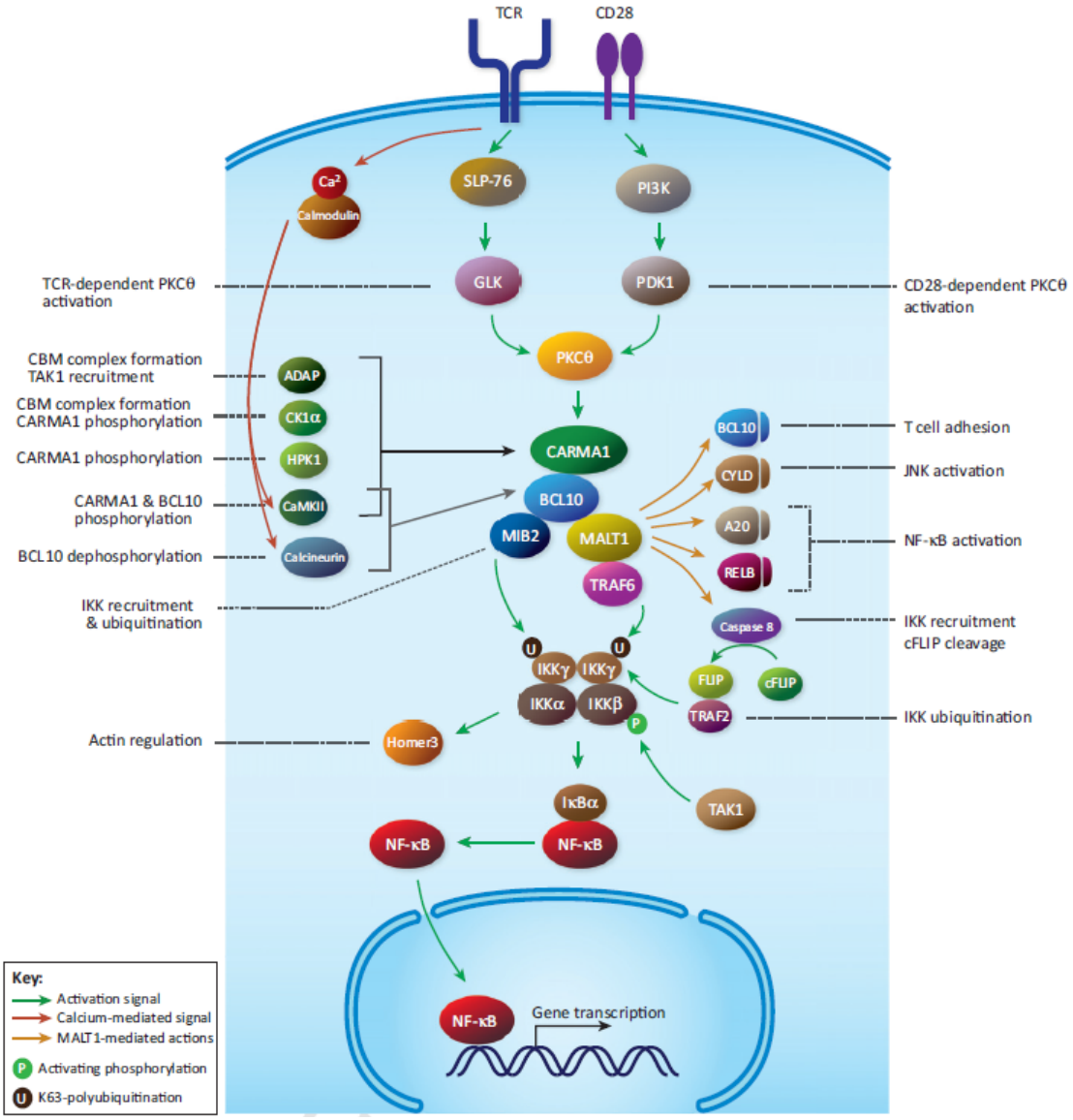

Introduction Figure. New developments in the T cell receptor (TCR)-to-nuclear factor (NF)-κB signaling pathway. The TCR transmits signals through the Q48 LAT–SLP76 complex, and possibly through GLK to activate protein kinase (PK)Cθ. CD28 signals through phosphoinositide 3-kinase (PI3K) and PDK1 to activate PKCθ. Activated PKCθ induces formation of the CARMA1, BCL10, MALT1 (CBM) complex. Newly identified proteins acting on CARMA1 and BCL10 are shown on the left. MALT1 enzymatic protein cleaving functions and caspase-8 recruitment are shown on the right. The CBM complex transmits activating signals to IκB kinase (IKK) through the ubiquitin ligases TRAF6, TRAF2 and/or MIB2. IKK phosphorylates IκBα leading to IκBα ubiquitination and degradation, allowing NF-κB nuclear translocation and gene transcription. (Figure adapted from "A new look at T cell receptor activation of NF-κB" by Suman Paul and Brian C Schaefer, *Trends in Immunology* in press)

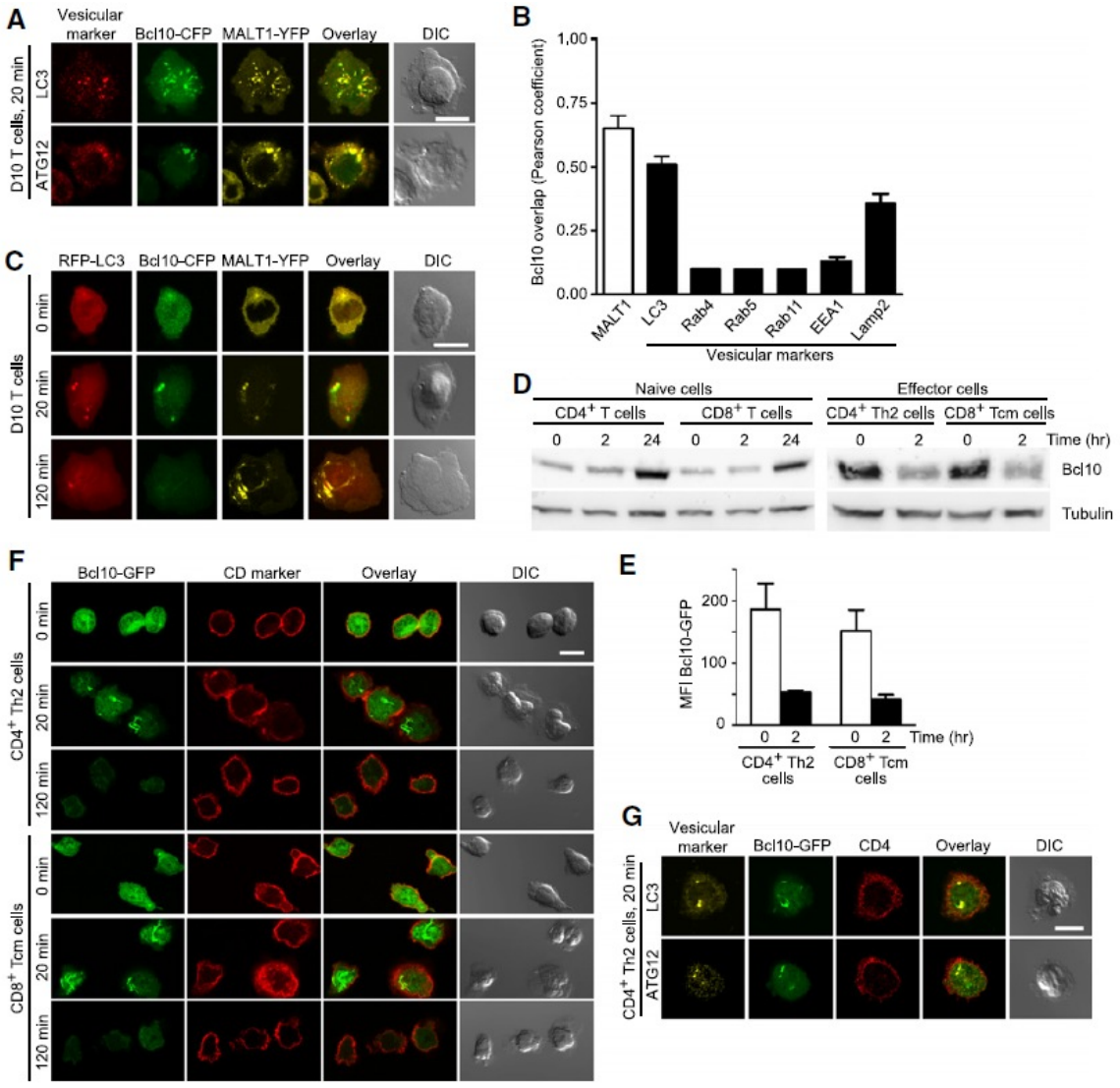

Figure 1 T cell activation leads to Bcl10 co-localization with markers of the autophagy-lysosomal degradation system and subsequent Bcl10 degradation. (A) D10 T cells expressing Bcl10-CFP and MALT1-YFP were stimulated with anti-CD3 for 20 min and stained with antibodies to the indicated autophagosome markers, to assess co-localization. (B) Pearson coefficient analysis was calculated by intensity correlation analysis of Bcl10-CFP fluorescence with MALT1-YFP fluorescence (white bar) or with fluorescence from antibodies specific for the indicated vesicular makers (black bars). For Pearson coefficient analysis, at least 30 cells were measured in each group. Values are means, error bars, SEM. (C) D10 T cells expressing RFP-LC3, Bcl10-CFP, and MALT1-YFP were stimulated with anti-CD3 and assessed by confocal microscopy for co-localization. (D) Primary naïve and effector T cells were stimulated with anti-CD3+anti-CD28 for the indicated times. Lysates were analyzed by immunoblotting for Bcl10 degradation. Blots were also probed with anti-α-tubulin as a loading control. Data are representative of two experiments. (E)

$CD4^+$ Th2 cells and $CD8^+$ Tcm cells expressing Bcl10-GFP were stimulated for the indicated times with CD3+anti-CD28. Flow cytometry was used to assess Bcl10-GFP degradation. Values are median Bcl10-GFP fluorescence (error bars, SEM), generated from three independent experiments. Representative flow cytometry histograms are shown in Supplemental Fig. 1C. (F,G) Primary effector T cells expressing Bcl10-GFP were stimulated with anti-CD3+anti-CD28 for the indicated times. Cells were stained with anti-CD4 or anti-CD8 to identify cell lineage (F); or with anti-LC3 and anti-ATG12 to assess co-localization with Bcl10-GFP (G). Images are representative of two independent experiments. Scale bar = 10μm. See also Figure S1.

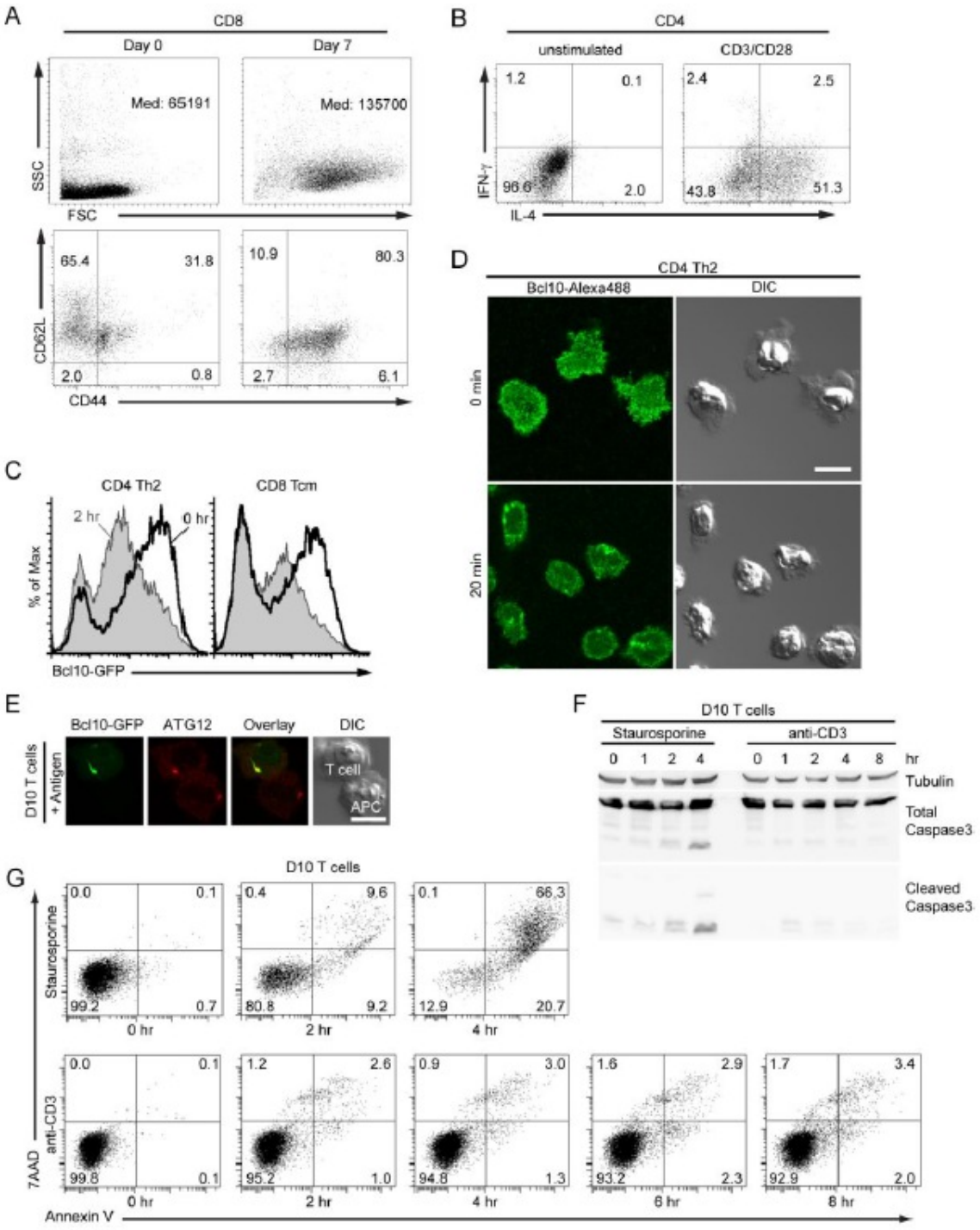

Figure S1Phenotype of in vitro generated effector T cells and analysis of cell death induction by anti-CD3. Flow cytometric analysis of $CD8_+$ T cells at the day of isolation (day 0) and 2 days after anti-CD3+anti-CD28 stimulation, followed by 5 days rest in IL-2 (day 7). (A) Dot plots showing forward scatter vs. side scatter, and CD62L vs. CD44, after gating on the$CD8_+$ population. (B) $CD4_+$ T

cells were stimulated for 4 days with anti-CD3+anti-CD28 plus IL-4, IL-2, anti-IFNY and anti-IL-12. After 2 days rest in IL-2, cells were unstimulated or stimulated for 6 hr with anti-CD3+anti-CD28 and analyzed by flow cytometry for intracellular IFN- and IL-4. Dot plots show cells after gating on the $CD4_+$ population. (C) Histogram of unstimulated (open plot) and 2 hr anti-CD3+anti CD28 stimulated (closed plot) $CD4_+$ Th2 cells and $CD8_+$ Tcm cells expressing Bcl10-GFP, to assess Bcl10-GFP degradation (leftward shift in peak). Data are representative of three independent experiments. (D) Primary $CD4_+$ Th2 cells were stimulated for the indicated times with anti-CD3+anti-CD28 and stained for endogenous Bcl10. Confocal microscopy was used to detect endogenous Bcl10 in POLKADOTS. (E) D10 T cells were stimulated for 20 min with CH12 B cells loaded with 250 g/mL conalbumin. Cells were stained with anti-ATG12, and Bcl10-GFP and endogenous ATG12 were visualized by confocal microscopy. Scale bars (D, E) = 10 m. (F & G) D10 T cells were treated with 1 M staurosporine (positive control to induce cell death) or activated with plate-bound anti CD3 for the indicated times, followed by immunoblotting with anti-(total) caspase 3 or anti-cleaved caspase 3 (F), or by 7-AAD plus annexin V staining with flow cytometry analysis to quantify T cell death (G). Numbers in quadrants (G) are percent cells in each region. Note that early cell death is detected in the annexin V_{high} $7AAD_{low}$ quadrant and late cell death is detected in the annexin V_{high} $7AAD_{high}$ quadrant.

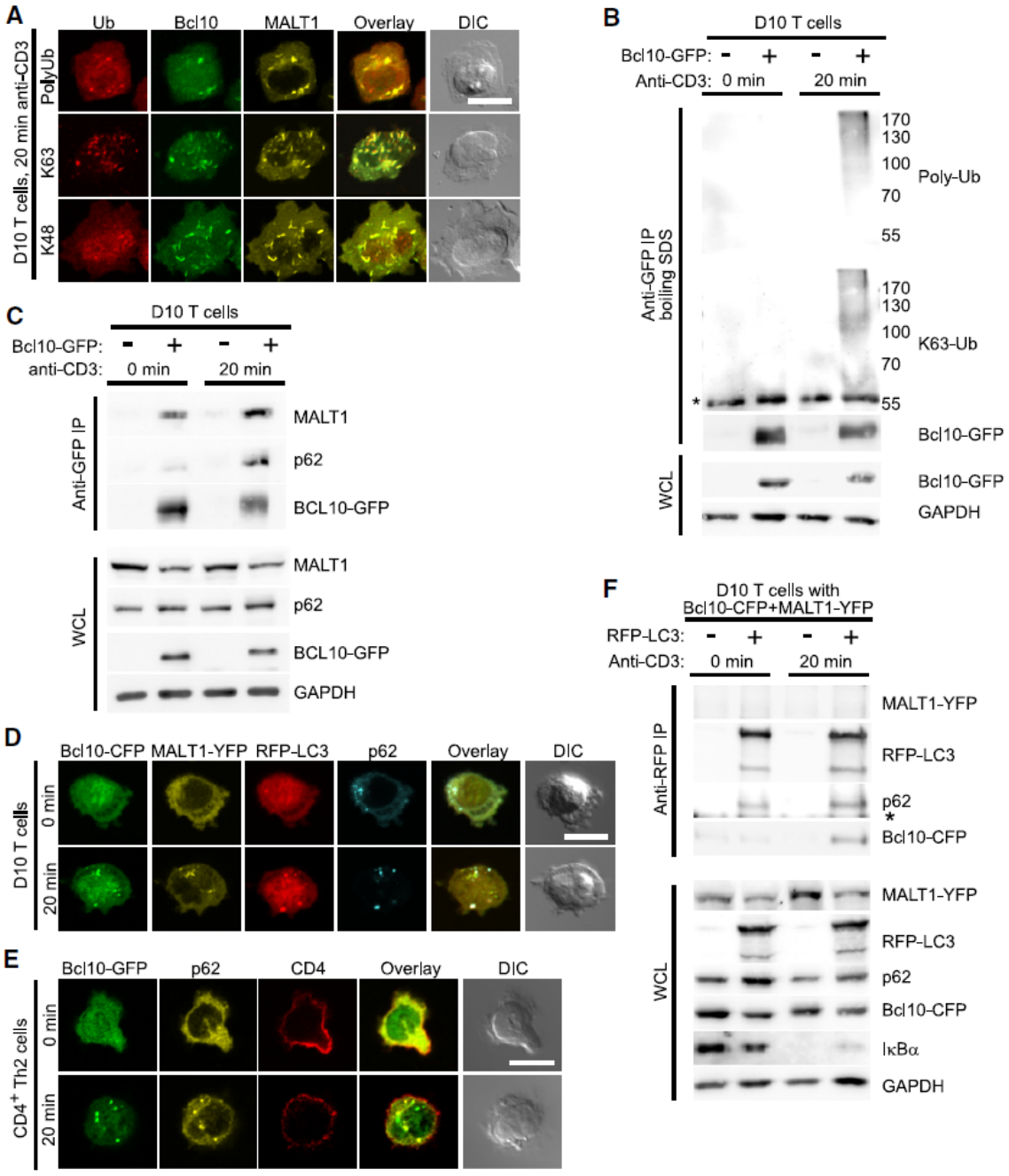

Figure 2 K63-polyubiquitinated Bcl10 interacts with p62. (A) D10 T cells expressing Bcl10-CFP and MALT1-YFP were stimulated for 20 min with anti-CD3, followed by staining with anti-polyubiquitin, anti-K48-polyubiquitin, or anti-K63-polyubiquitin. (B) Unstimulated or anti-CD3 stimulated D10 T cells with or without Bcl10-GFP were lysed and heated at 95ºC for 5 min with 1% SDS to disrupt protein-protein interactions. Bcl10-GFP was immunoprecipitated using anti-GFP, followed by immunoblot analysis to detect Bcl10-GFP ubiquitination. (C) D10 T cells expressing or not expressing Bcl10-GFP were stimulated with anti-CD3 for the indicated times and lysed. Bcl10-GFP was recovered by

immunoprecipitation using anti-GFP, followed by immunoblot analysis with the indicated antibodies to detect Bcl10 binding partners. (D) Confocal microscopy analysis of D10 T cells expressing Bcl10-CFP, MALT1-YFP, RFP-LC3, with 0 or 20 min anti-CD3 stimulation, to assess co-localization between proteins. (E) $CD4^+$ Th2 cells expressing Bcl10-GFP were stimulated for the indicated times with anti-CD3+anti-CD28. Cells were stained with anti-p62 and anti-CD4, and confocal microscopy was used to assess co-localization between Bcl10 and p62. (F) D10 T cells expressing Bcl10-CFP and MALT1-YFP, with or without RFP-LC3, were stimulated for the indicated times with anti-CD3. Cells were lysed and RFP-LC3 was immunoprecipitated, using anti-RFP. Immunoblotting with the indicated antibodies was used to detect LC3 binding partners. (*) indicates position of Ig heavy chain. WCL, whole cell lysates; Ub, ubiquitin. Scale bar = 10μm. Data representative of two (B,C,F) or three (A,D,E) independent experiments. See also Figure S2.

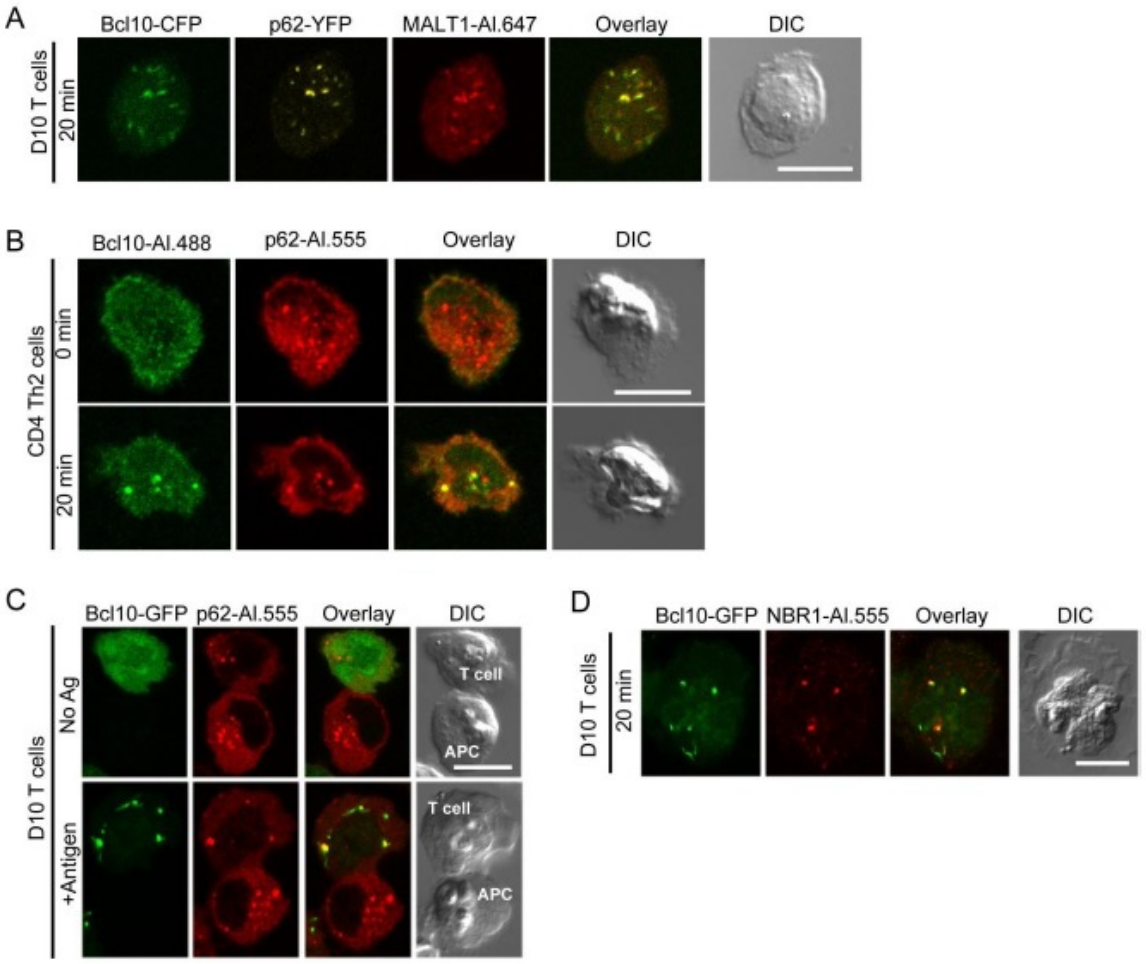

Figure S2 p62 co-localizes with Bcl10 clusters (POLKADOTS) and NBR1. (A) D10 T cells expressing Bcl10-CFP and p62-YFP were stimulated with anti-CD3 for 20 min. Cells were stained with anti-MALT1 and assessed by confocal microscopy for co-localization between proteins. (B) $CD4_+$ Th2 cells were stimulated with anti-CD3+anti-CD28 for the indicated times and stained with anti-Bcl10 and anti-p62. Cells were analyzed by confocal microscopy for co-localization between p62 and Bcl10. (C) D10 T cells were stimulated for 20 min with CH12 B cells loaded with no antigen (No Ag) or with 250 g/mL conalbumin (+ Antigen). Cells were stained with anti-p62, followed by an Alexa-555 secondary antibody (Al.555). Bcl10-GFP and endogenous p62 were visualized by confocal microscopy. (D) D10 T cells expressing Bcl10-GFP were stimulated with anti-CD3 for 20 min. Cells were stained with an anti-NBR1, followed by an Alexa-555 secondary antibody (Al.555), and imaged by confocal microscopy to assess colocalization between Bcl10 and NBR1. Scale bar = 10 m.

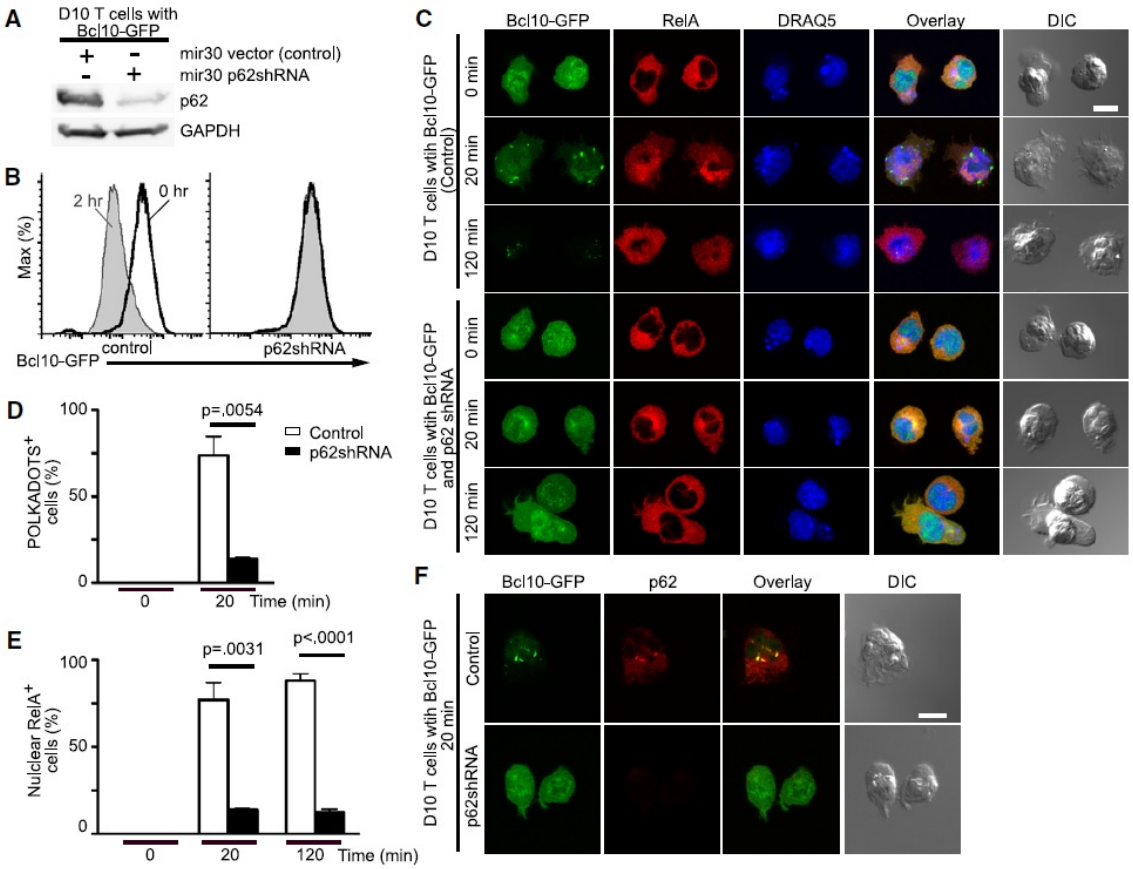

Figure 3 p62 silencing inhibits RelA nuclear translocation and blocks Bcl10 degradation. (A) D10 T cells expressing Bcl10-GFP plus either mir30 shRNA vector or mir30 p62shRNA were analyzed by immunoblotting to detect p62 expression. (B-E) D10 T cells expressing Bcl10-GFP plus mir30 shRNA vector or mir30 p62shRNA were stimulated with anti-CD3 for the indicated times. Cells were analyzed by flow cytometry to detect degradation of Bcl10-GFP (B); or stained with anti-RelA and the DNA dye, DRAQ5, and analyzed by confocal microscopy to assess RelA nuclear translocation (C). Graphs showing percentage of cells in (C) forming Bcl10-GFP clusters (POLKADOTS) (D) or with RelA nuclear translocation (E). (F) D10 T cells expressing Bcl10-GFP plus mir30 shRNA vector or mir30 p62shRNA were stimulated for 20 min with anti-CD3 and stained with anti-p62. p62 degradation and p62-Bcl10 co-localization were assessed by confocal microscopy. Means (+/- SEM) were calculated by counting at least 20 cells from each of three experiments. Scale bar = 10μm. Data are representative of two (A,B) or three (C,F) independent experiments. See also Figure S3.

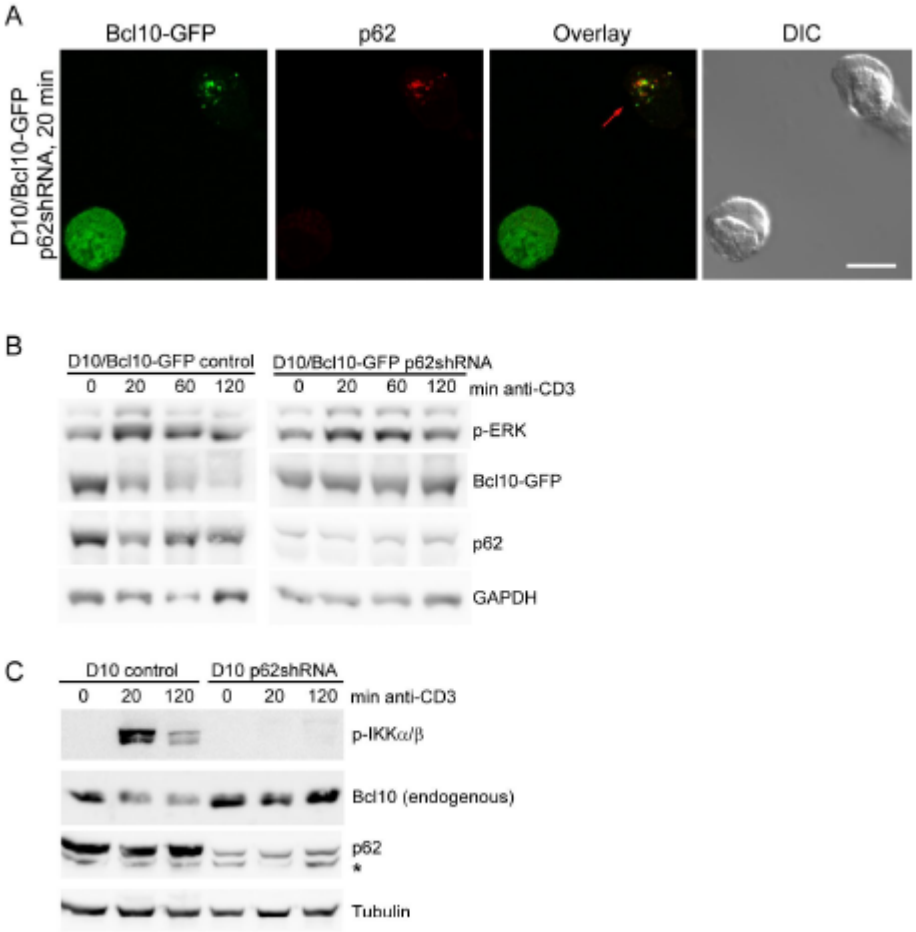

Figure S3. p62 silencing inhibits formation of Bcl10 POLKADOTS and blocks IKK activation, but does not affect ERK1/2 phosphorylation. (A) D10 T cells expressing Bcl10-GFP (D10/Bcl10-GFP) and p62shRNA were stimulated with anti-CD3 for 20 min, stained with anti-p62, and analyzed by confocal microscopy. Red arrow points to a cell with residual p62 expression, which also demonstrates Bcl10-GFP clustering. There is no clustering of Bcl10-GFP in cells with efficient p62 silencing. (B) D10 T cells expressing Bcl10-GFP and infected with the empty shRNA vector (D10/Bcl10-GFP control) or expressing Bcl10-GFP and infected with the p62shRNA vector (D10/Bcl10-GFP p62shRNA) were stimulated for the indicated times with anti-CD3. Cells were analyzed by immunoblotting for Bcl10-GFP degradation, phosphorylation of ERK1 and ERK2, silencing of p62, and for levels of GAPDH (a loading control). (C) D10 T cells infected with the empty shRNA vector (control) or with the vector expressing the p62shRNA were stimulated for the indicated times with anti-CD3. Cells were analyzed by immunoblotting for endogenous Bcl10 degradation, IKK / phosphorylation, p62 silencing, and Tubulin expression (loading control). * indicates non-specific band. Scale bar = 10 m.

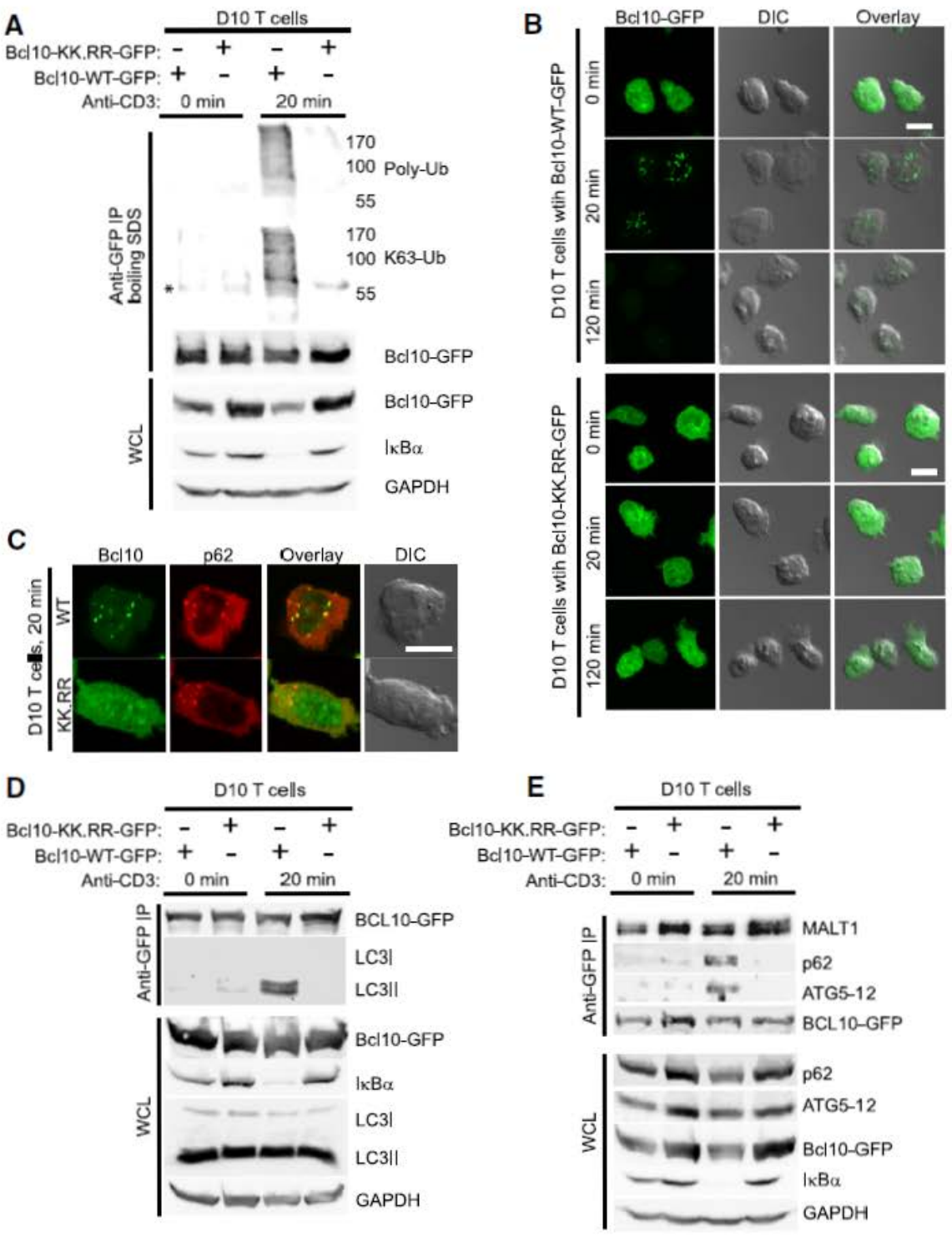

Figure 4 Inhibition of Bcl10 K63-polyubiquitination blocks Bcl10 clustering and degradation. (A) Unstimulated or anti-CD3 stimulated D10 T cells expressing either wild-type or the K31R,K63R mutant of Bcl10-GFP (Bcl10-WT-GFP and Bcl10-KK.RR-GFP, respectively) were lysed and heated at 95ºC in 1% SDS for 5 min to disrupt protein complexes. Bcl10-GFP was immunoprecipitated using

anti-GFP, followed by immunoblotting analysis to detect Bcl10 ubiquitination. (B,C) D10 T cells expressing either Bcl10-WT-GFP or Bcl10-KK.RR-GFP were stimulated for the indicated times with anti-CD3 and analyzed by confocal microscopy. Cells were assessed for redistribution of Bcl10-GFP in POLKADOTS (B) and for Bcl10-p62 co-localization via staining with anti-p62 (C). (D,E) D10 T cells expressing either Bcl10-WT-GFP or Bcl10-KK.RR-GFP were stimulated for the indicated times with anti-CD3, followed by lysis and immunoprecipitation using anti-GFP. Immunoblotting was used to detect Bcl10 association with LC3 (D) and with p62 and Atg5-12 (E). (*) indicates position of Ig heavy chain. Scale bar = 10μm. Data are representative of two (A,D,E) or three experiments (B,C). See also Figure S4.

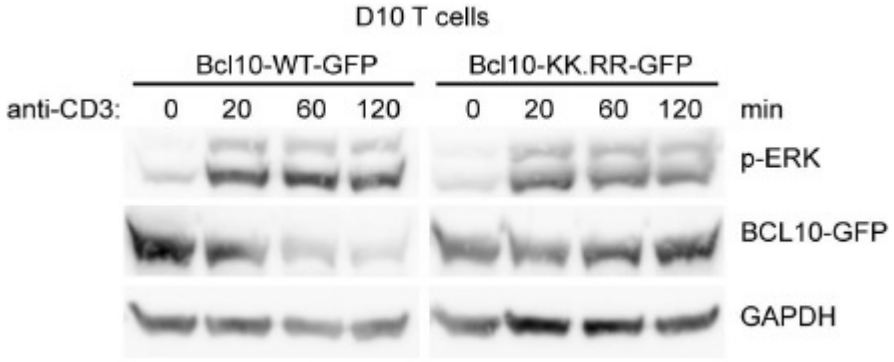

Figure S4 Inhibition of Bcl10 K63-polyubiquitination does not affect ERK1 and ERK2 phosphorylation. D10 T cells expressing either Bcl10-WT-GFP or Bcl10-KK.RR-GFP were stimulated with anti-CD3 for the indicated times. Cells were lysed and assessed by immunoblotting for ERK phosphorylation, Bcl10 degradation, and GAPDH levels.

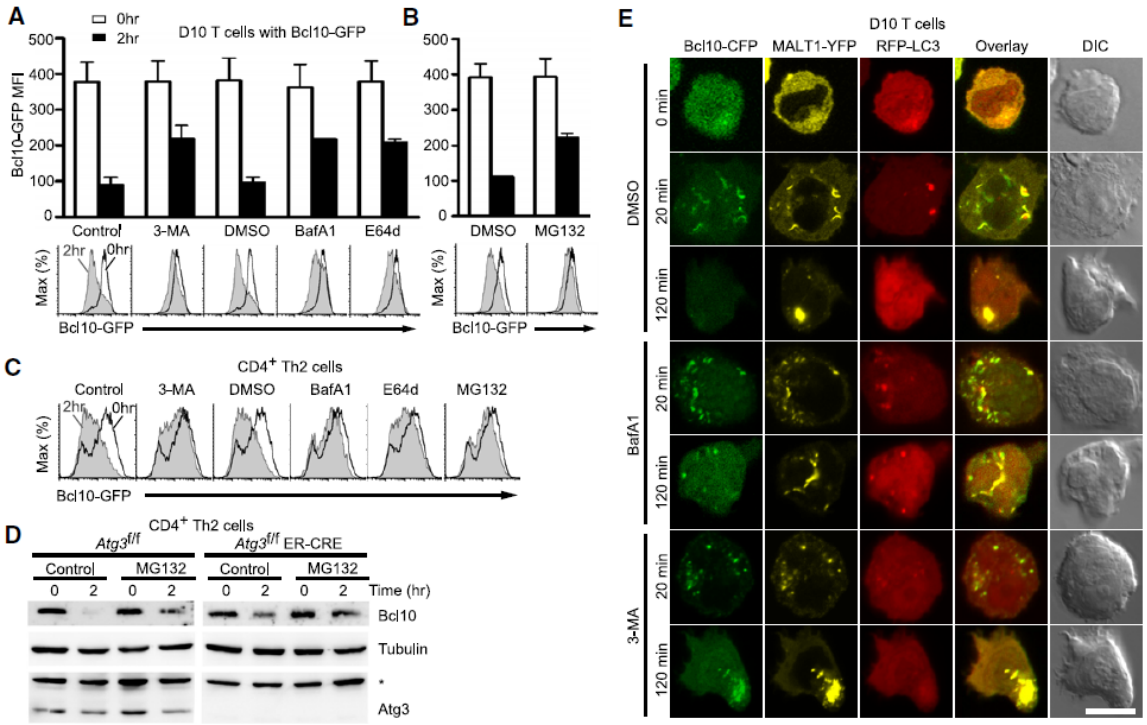

Figure 5 Blockade of autophagy prevents TCR-dependent Bcl10 degradation. D10 T cells (A,B) expressing Bcl10-GFP were pre-treated with distilled water (control), DMSO (vehicle control), the autophagy inhibitor 3-methyladenine (3-MA), or the lysosomal degradation inhibitors Bafilomycin A1 (BafA1) and E64d (A) or the proteasomal inhibitor MG132 (B), and stimulated for the indicated times with anti-CD3. Bcl10-GFP degradation was assessed by flow cytometry. Histograms are representative data from one experiment and bar graphs are mean (+/-SEM.) of Bcl10-GFP median fluorescence intensity (MFI) from three independent experiments. (C) The experiment of (A) and (B) was repeated using primary Th2 cells. (D) Primary Th2 cells expressing (*Atg3*$^{f/f}$) or not expressing ATG3 (*Atg3*$^{f/f}$ ER-Cre) were pretreated with vehicle (control) or MG132, followed anti-CD3+anti-CD28 stimulation for the indicated times. Endogenous Bcl10, tubulin, and ATG3 were detected by immunoblotting. (E) D10 T cells expressing Bcl10-CFP, MALT1-YFP and RFP-LC3 were pre-treated with DMSO (control), BafA1, or 3-MA, followed by anti-CD3 stimulation. Cells were imaged by confocal microscopy to assess co-localization between proteins. Data are representative of two independent experiments. Scale bar = 10μm.

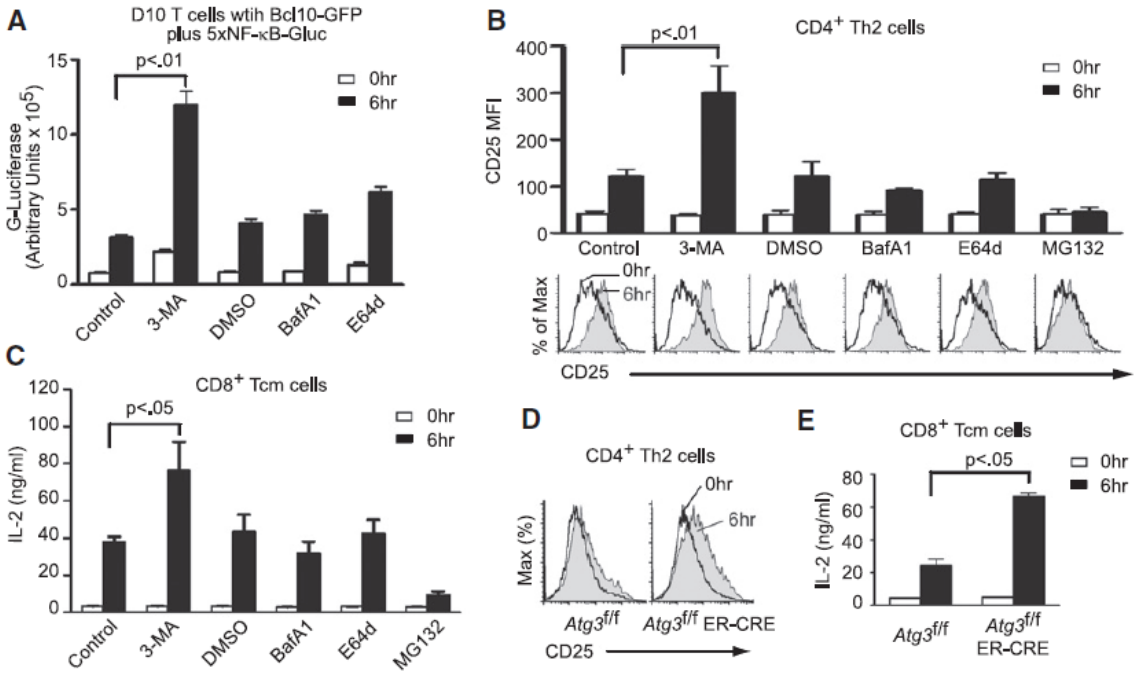

Figure 6 Blockade of autophagy enhances TCR-mediated NF-κB activation. (A) D10 T cells expressing Bcl10-GFP plus an integrated 5×NF-κB Gaussia luciferase reporter were pre-treated with indicated inhibitors. Cells were stimulated with anti-CD3 for the indicated times, and supernatants were harvested. Graph shows mean secreted luciferase activity (+/- SEM). (B) $CD4^+$ Th2 cells were pre-treated with the indicated compounds and stimulated with anti-CD3+anti-CD28 for the indicated times. Cells were analyzed by flow cytometry to measure induction of CD25 expression after gating on the CD4 positive population (>90%). Histograms are representative data from one experiment and bar graphs are means (+/- SEM) of anti-CD25 fluorescence generated from three independent experiments. (C) The experiment of (B) was repeated with $CD8^+$ Tcm cells, and secreted IL-2 was measured by XTT assay. Bar graphs are means, +/- SEM. (D) Primary Th2 cells expressing (*Atg3*$^{f/f}$) or not expressing ATG3 (*Atg3*$^{f/f}$ ER-Cre) were stimulated for 6 hr with anti-CD3+anti-CD28 and analyzed by flow cytometry for CD25 expression. (E) The experiment of (D) was repeated with $CD8^+$ Tcm cells, and secreted IL-2 was measured by XTT assay. Bar graphs are means (+/- SEM). Data are representative of two independent experiments (C-E).

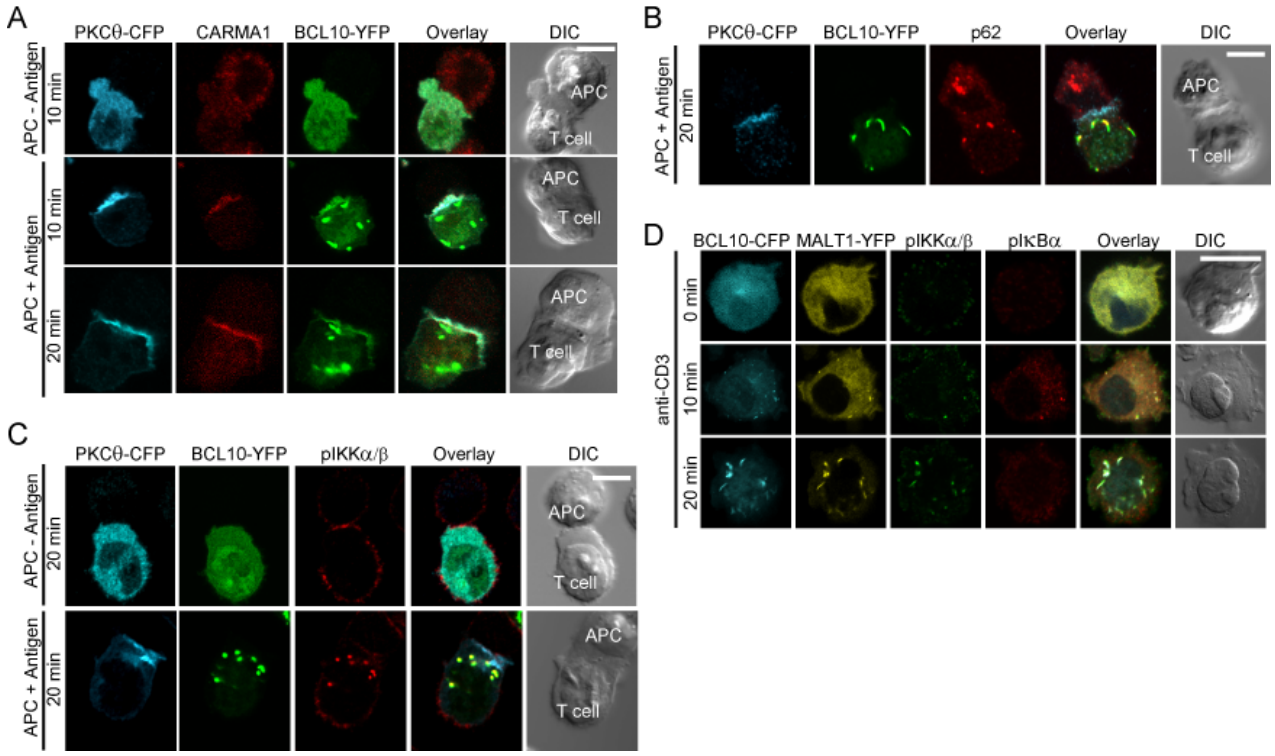

Figure 7. Cytosolic Bcl10-p62 clusters/signalosomes are sites of IKK and IκBα phosphorylation in effector T cells. (A-C) Confocal images of unstimulated (- Antigen) or stimulated (+ Antigen) D10 T cells expressing PKCθ-CFP and Bcl10-YFP, fixed at indicated time points and stained with the following antibodies: (A) Carma1-Alexa647 or (B) p62-Alexa647 or (C) phospho-IKKα/β-Alexa647. (D) Confocal images of anti-CD3 stimulated D10 T cells expressing Bcl10-CFP and Malt-YFP, fixed at the indicated time points and stained with anti-phospho-IKKα/β-Alexa555 and anti-phospho-IκBα-Alexa647. Images are representative of three (A and D) or four (B and C) independent experiments. Scale bar represents 10 μm.

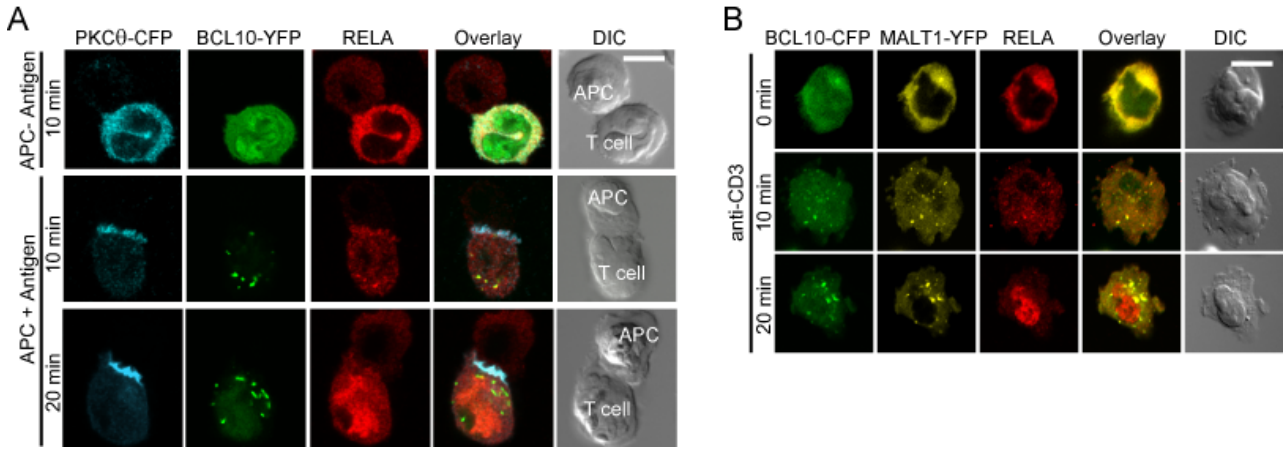

Figure 8. RelA transiently co-localizes with cytosolic Bcl10 signalosomes before translocating to the nucleus. (A) Confocal images of unstimulated (- Antigen) or stimulated (+ Antigen) D10 T cells expressing PKCθ-CFP and Bcl10-YFP, fixed at the indicated time points and stained with anti-RelA-Alexa647. (B) Confocal images of anti-CD3 stimulated D10 T cells expressing Bcl10-CFP and Malt1-YFP, fixed at the indicated times and stained with anti-RelA-Alexa647. Images representative of at least four independent experiments. Scale bar represents 10μm.

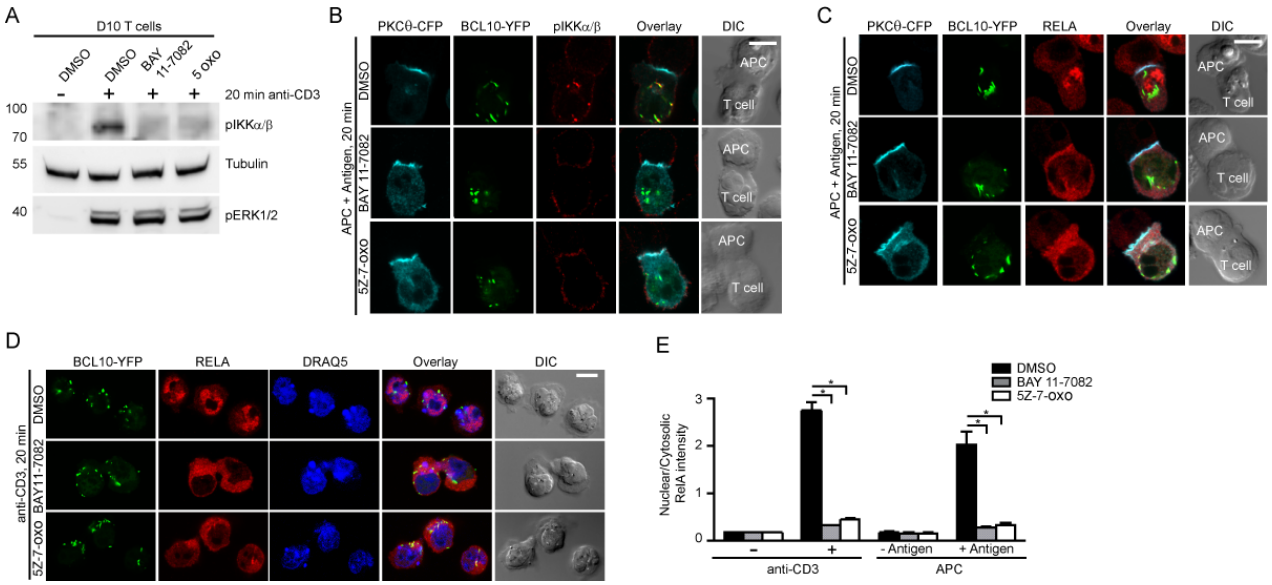

Figure 9. Pharmacological inhibitors block IKK phosphorylation at cytosolic Bcl10 signalosomes, causing reduced RelA activation. (A) D10 T cells treated with DMSO (control), or BAY 11-7082, or 5Z-7-oxozeaenol, stimulated with anti-CD3 for 20 min, lysed and western blotted with antibodies against proteins indicated on right. Numbers on left indicate location of molecular weight markers in kDa. (B to D) Confocal images of DMSO or BAY 11-7082 or 5Z-7-oxozeaenol-treated D10 T cells expressing PKCθ-CFP and Bcl10-YFP, stimulated with APC + Antigen (B and C) or anti-CD3 (D) for 20 min, fixed and stained with antibody against (B) phospho-IKKα/β-Alexa647 or (C and D) RelA-Alexa647. DRAQ5 used to stain nuclear DNA in (D). (E) The nuclear and cytosolic RelA signal was quantified from experiments performed in (C) and (D). The bar graph was generated by plotting the ratio of nuclear to cytosolic RelA signal from each group. At least 20 cells were counted in each group. * p value <.05. Images are representative of three independent experiments (B-C). Scale bar represents 10 μm. 5Z-7-oxo, 5Z-7-oxozeaenol.

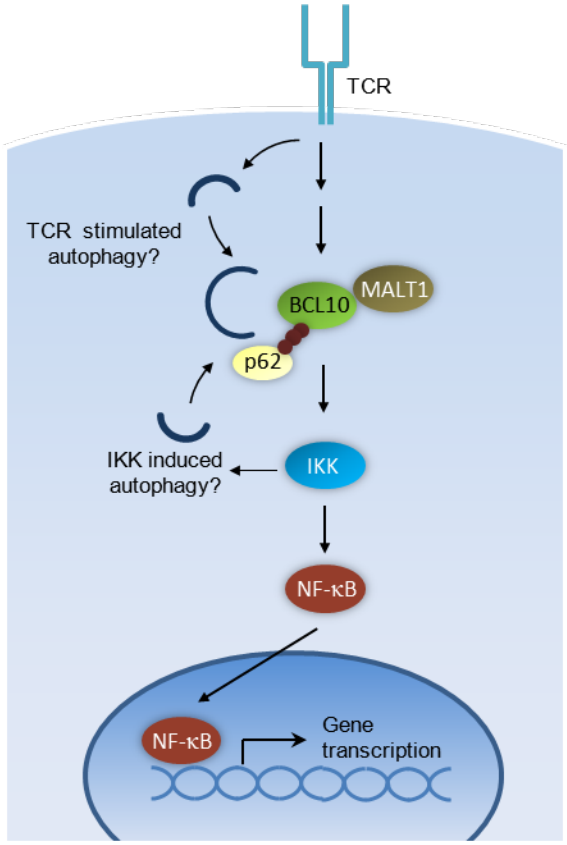

Figure 10. Mechanism of T cell activation and autophagic Bcl10 degradation in effector T cells. Bcl10 can initiate autophagosome formation by activating IKK, a known inducer of autophagy. Alternatively, an unknown TCR dependent activation of autophagy, may be responsible for Bcl10 degradation. (Figure adapted from "Selective autophagy regulates T cell activation" by Suman Paul and Brian C Schaefer, *Autophagy, 2012 Nov 1;8(11):1690-2*)

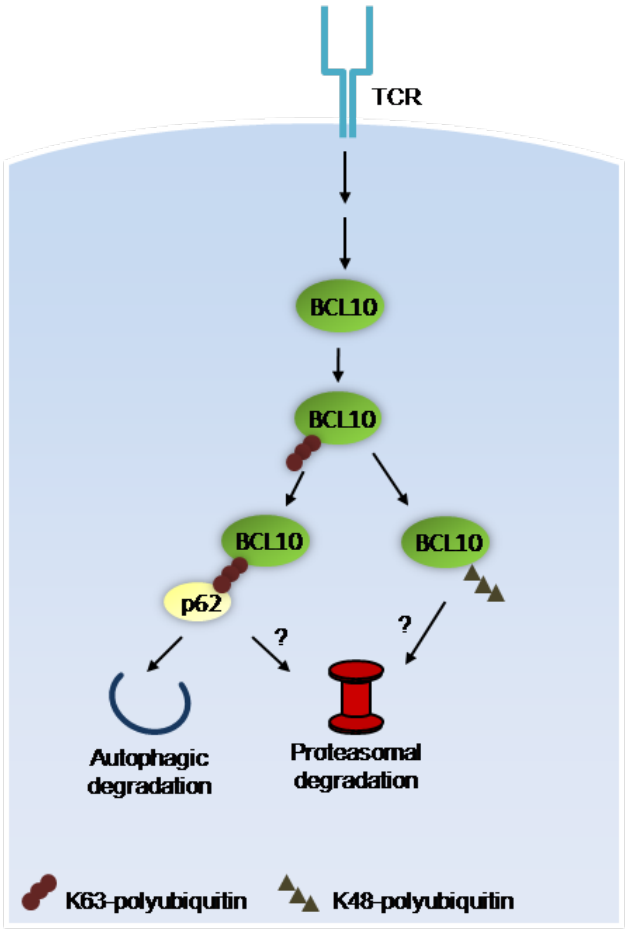

Figure11.Mechanism of autophagic and proteasomal degradation of Bcl10. K63-polyubiquitinated Bcl10 binds p62 and can be directed into both autophagosomes and proteasomes. Alternatively, ubiquitin editing of Bcl10 can convert the K63 to K48- linked polyubiquitin, followed by channeling of K48-polyubiquitinated Bcl10 towards proteasomes for degradation. (Figure adapted from "Selective autophagy regulates T cell activation" by Suman Paul and Brian C Schaefer, *Autophagy, 2012 Nov 1;8(11):1690-2*)

REFERENCES

1. Ballard DW, Bohnlein E, Lowenthal JW, Wano Y, Franza BR, Greene WC. 1988. HTLV-I tax induces cellular proteins that activate the kappa B element in the IL-2 receptor alpha gene. *Science* 241:1652-5
2. Bidere N, Snow AL, Sakai K, Zheng L, Lenardo MJ. 2006. Caspase-8 regulation by direct interaction with TRAF6 in T cell receptor-induced NF-kappaB activation. *Current biology : CB* 16:1666-71
3. Cartwright NG, Kashyap AK, Schaefer BC. 2011. An active kinase domain is required for retention of PKCtheta at the T cell immunological synapse. *Mol Biol Cell* 22:3491-7
4. Carvalho G, Le Guelte A, Demian C, Vazquez A, Gavard J, Bidere N. 2010. Interplay between BCL10, MALT1 and IkappaBalpha during T-cell-receptor-mediated NFkappaB activation. *J Cell Sci* 123:2375-80
5. Carvalho G, Le Guelte A, Demian C, Vazquez A, Gavard J, Bidere N. 2010. Interplay between BCL10, MALT1 and IkappaBalpha during T-cell-receptor-mediated NFkappaB activation. *Journal of cell science* 123:2375-80
6. Chaturvedi A, Pierce SK. 2009. Autophagy in immune cell regulation and dysregulation. *Curr Allergy Asthma Rep* 9:341-6
7. Chuang HC, Lan JL, Chen DY, Yang CY, Chen YM, et al. 2011. The kinase GLK controls autoimmunity and NF-kappaB signaling by activating the kinase PKC-theta in T cells. *Nature immunology* 12:1113-8
8. Coornaert B, Baens M, Heyninck K, Bekaert T, Haegman M, et al. 2008. T cell antigen receptor stimulation induces MALT1 paracaspase-mediated cleavage of the NF-kappaB inhibitor A20. *Nat Immunol* 9:263-71
9. Criollo A, Senovilla L, Authier H, Maiuri MC, Morselli E, et al. 2010. The IKK complex contributes to the induction of autophagy. *EMBO J* 29:619-31
10. Dustin ML, Chakraborty AK, Shaw AS. 2010. Understanding the structure and function of the immunological synapse. *Cold Spring Harbor perspectives in biology* 2:a002311
11. Duwel M, Welteke V, Oeckinghaus A, Baens M, Kloo B, et al. 2009. A20 negatively regulates T cell receptor signaling to NF-kappaB by cleaving Malt1 ubiquitin chains. *J Immunol* 182:7718-28
12. Duwel M, Welteke V, Oeckinghaus A, Baens M, Kloo B, et al. 2009. A20 negatively regulates T cell receptor signaling to NF-kappaB by cleaving Malt1 ubiquitin chains. *Journal of immunology* 182:7718-28
13. Faroudi M, Zaru R, Paulet P, Muller S, Valitutti S. 2003. Cutting edge: T lymphocyte activation by repeated immunological synapse formation and intermittent signaling. *Journal of immunology* 171:1128-32
14. Fitch FW, Gajewski TF, Hu-Li J. 2006. Production of TH1 and TH2 cell lines and clones. *Curr Protoc Immunol* Chapter 3:Unit 3 13
15. Gaide O, Favier B, Legler DF, Bonnet D, Brissoni B, et al. 2002. CARMA1 is a critical lipid raft-associated regulator of TCR-induced NF-kappa B activation. *Nature immunology* 3:836-43

16. Gao C, Cao W, Bao L, Zuo W, Xie G, et al. 2010. Autophagy negatively regulates Wnt signalling by promoting Dishevelled degradation. *Nat Cell Biol* 12:781-90
17. Gunzer M, Schafer A, Borgmann S, Grabbe S, Zanker KS, et al. 2000. Antigen presentation in extracellular matrix: interactions of T cells with dendritic cells are dynamic, short lived, and sequential. *Immunity* 13:323-32
18. Hailfinger S, Lenz G, Ngo V, Posvitz-Fejfar A, Rebeaud F, et al. 2009. Essential role of MALT1 protease activity in activated B cell-like diffuse large B-cell lymphoma. *Proceedings of the National Academy of Sciences of the United States of America* 106:19946-51
19. Hailfinger S, Nogai H, Pelzer C, Jaworski M, Cabalzar K, et al. 2011. Malt1-dependent RelB cleavage promotes canonical NF- B activation in lymphocytes and lymphoma cell lines. *Proceedings of the National Academy of Sciences* 108:14596-601
20. Hou F, Sun L, Zheng H, Skaug B, Jiang QX, Chen ZJ. 2011. MAVS forms functional prion-like aggregates to activate and propagate antiviral innate immune response. *Cell* 146:448-61
21. Hoyos B, Ballard DW, Bohnlein E, Siekevitz M, Greene WC. 1989. Kappa B-specific DNA binding proteins: role in the regulation of human interleukin-2 gene expression. *Science* 244:457-60
22. Hu S, Du MQ, Park SM, Alcivar A, Qu L, et al. 2006. cIAP2 is a ubiquitin protein ligase for BCL10 and is dysregulated in mucosa-associated lymphoid tissue lymphomas. *J Clin Invest* 116:174-81
23. Iezzi G, Karjalainen K, Lanzavecchia A. 1998. The duration of antigenic stimulation determines the fate of naive and effector T cells. *Immunity* 8:89-95
24. Inomata M, Niida S, Shibata K, Into T. 2012. Regulation of Toll-like receptor signaling by NDP52-mediated selective autophagy is normally inactivated by A20. *Cell Mol Life Sci* 69:963-79
25. Jia W, He YW. 2011. Temporal regulation of intracellular organelle homeostasis in T lymphocytes by autophagy. *J Immunol* 186:5313-22
26. Jia W, He YW. 2011. Temporal regulation of intracellular organelle homeostasis in T lymphocytes by autophagy. *Journal of immunology* 186:5313-22
27. Jia W, Pua HH, Li QJ, He YW. 2011. Autophagy regulates endoplasmic reticulum homeostasis and calcium mobilization in T lymphocytes. *J Immunol* 186:1564-74
28. Karin M, Greten FR. 2005. NF-kappaB: linking inflammation and immunity to cancer development and progression. *Nat Rev Immunol* 5:749-59
29. Kingeter LM, Paul S, Maynard SK, Cartwright NG, Schaefer BC. 2010. Cutting edge: TCR ligation triggers digital activation of NF-kappaB. *Journal of immunology* 185:4520-4
30. Kingeter LM, Paul S, Maynard SK, Cartwright NG, Schaefer BC. 2010. Cutting edge: TCR ligation triggers digital activation of NF-kappaB. *J Immunol* 185:4520-4
31. Kingeter LM, Schaefer BC. 2008. Loss of protein kinase C theta, Bcl10, or Malt1 selectively impairs proliferation and NF-kappa B activation in the CD4+ T cell subset. *J Immunol* 181:6244-54

32. Kingeter LM, Schaefer BC. 2008. Loss of protein kinase C theta, Bcl10, or Malt1 selectively impairs proliferation and NF-kappa B activation in the CD4+ T cell subset. *J Immunol* 181:6244-54
33. Kirkin V, Lamark T, Sou YS, Bjorkoy G, Nunn JL, et al. 2009. A role for NBR1 in autophagosomal degradation of ubiquitinated substrates. *Mol Cell* 33:505-16
34. Kirkin V, McEwan DG, Novak I, Dikic I. 2009. A role for ubiquitin in selective autophagy. *Mol Cell* 34:259-69
35. Klionsky DJ, Elazar Z, Seglen PO, Rubinsztein DC. 2008. Does bafilomycin A1 block the fusion of autophagosomes with lysosomes? *Autophagy* 4:849-950
36. Kraft C, Peter M, Hofmann K. 2010. Selective autophagy: ubiquitin-mediated recognition and beyond. *Nat Cell Biol* 12:836-41
37. Krishna S, Xie D, Gorentla B, Shin J, Gao J, Zhong XP. 2012. Chronic activation of the kinase IKKbeta impairs T cell function and survival. *Journal of immunology* 189:1209-19
38. Levine B, Mizushima N, Virgin HW. 2011. Autophagy in immunity and inflammation. *Nature* 469:323-35
39. Li C, Capan E, Zhao Y, Zhao J, Stolz D, et al. 2006. Autophagy is induced in CD4+ T cells and important for the growth factor-withdrawal cell death. *J Immunol* 177:5163-8
40. Lobry C, Lopez T, Israel A, Weil R. 2007. Negative feedback loop in T cell activation through IkappaB kinase-induced phosphorylation and degradation of Bcl10. *PNAS* 104:908-13
41. Lunemann JD, Munz C. 2009. Autophagy in CD4+ T-cell immunity and tolerance. *Cell Death Differ* 16:79-86
42. Manjunath N, Shankar P, Wan J, Weninger W, Crowley MA, et al. 2001. Effector differentiation is not prerequisite for generation of memory cytotoxic T lymphocytes. *J Clin Invest* 108:871-8
43. Martin P, Diaz-Meco MT, Moscat J. 2006. The signaling adapter p62 is an important mediator of T helper 2 cell function and allergic airway inflammation. *Embo J* 25:3524-33
44. Mizushima N. 2007. Autophagy: process and function. *Genes Dev* 21:2861-73
45. Moreno-Garcia ME, Sommer K, Haftmann C, Sontheimer C, Andrews SF, Rawlings DJ. 2009. Serine 649 phosphorylation within the protein kinase C-regulated domain down-regulates CARMA1 activity in lymphocytes. *Journal of immunology* 183:7362-70
46. Moscat J, Diaz-Meco MT. 2009. p62 at the crossroads of autophagy, apoptosis, and cancer. *Cell* 137:1001-4
47. Moscat J, Diaz-Meco MT, Wooten MW. 2009. Of the atypical PKCs, Par-4 and p62: recent understandings of the biology and pathology of a PB1-dominated complex. *Cell Death Differ* 16:1426-37
48. Palombella VJ, Rando OJ, Goldberg AL, Maniatis T. 1994. The ubiquitin-proteasome pathway is required for processing the NF-kappa B1 precursor protein and the activation of NF-kappa B. *Cell* 78:773-85
49. Park SG, Schulze-Luehrman J, Hayden MS, Hashimoto N, Ogawa W, et al. 2009. The kinase PDK1 integrates T cell antigen receptor and CD28 coreceptor

signaling to induce NF-kappaB and activate T cells. *Nature immunology* 10:158-66

50. Paul S, Kashyap AK, Jia W, He YW, Schaefer BC. 2012. Selective autophagy of the adaptor protein Bcl10 modulates T cell receptor activation of NF-kappaB. *Immunity* 36:947-58
51. Paul S, Schaefer BC. 2013. A new look at T cell receptor signaling to nuclear factor-kappaB. *Trends Immunol*
52. Pua HH, Dzhagalov I, Chuck M, Mizushima N, He YW. 2007. A critical role for the autophagy gene Atg5 in T cell survival and proliferation. *J Exp Med* 204:25-31
53. Purbhoo MA, Irvine DJ, Huppa JB, Davis MM. 2004. T cell killing does not require the formation of a stable mature immunological synapse. *Nature immunology* 5:524-30
54. Rebeaud F, Hailfinger S, Posevitz-Fejfar A, Tapernoux M, Moser R, et al. 2008. The proteolytic activity of the paracaspase MALT1 is key in T cell activation. *Nat Immunol* 9:272-81
55. Reggiori F, Komatsu M, Finley K, Simonsen A. 2012. Autophagy: more than a nonselective pathway. *Int J Cell Biol* 2012:219625
56. Rossman JS, Stoicheva NG, Langel FD, Patterson GH, Lippincott-Schwartz J, Schaefer BC. 2006. POLKADOTS are foci of functional interactions in T-Cell receptor-mediated signaling to NF-kappaB. *Mol Biol Cell* 17:2166-76
57. Ruland J, Duncan GS, Elia A, del Barco Barrantes I, Nguyen L, et al. 2001. Bcl10 is a positive regulator of antigen receptor-induced activation of NF-kappaB and neural tube closure. *Cell* 104:33-42
58. Saunders RN, Metcalfe MS, Nicholson ML. 2001. Rapamycin in transplantation: a review of the evidence. *Kidney Int* 59:3-16
59. Schaefer BC, Kappler JW, Kupfer A, Marrack P. 2004. Complex and dynamic redistribution of NF-kappaB signaling intermediates in response to T cell receptor stimulation. *Proceedings of the National Academy of Sciences of the United States of America* 101:1004-9
60. Scharschmidt E, Wegener E, Heissmeyer V, Rao A, Krappmann D. 2004. Degradation of Bcl10 induced by Tcell activation negatively regulates NF-kappaB signaling. *Molecular and Cellular Biology* 24:3860-73
61. Schulze-Luehrmann J, Ghosh S. 2006. Antigen-receptor signaling to nuclear factor kappa B. *Immunity* 25:701-15
62. Sebald A, Mattioli I, Schmitz ML. 2005. T cell receptor-induced lipid raft recruitment of the I kappa B kinase complex is necessary and sufficient for NF-kappa B activation occurring in the cytosol. *European journal of immunology* 35:318-25
63. Seglen PO, Gordon PB. 1982. 3-Methyladenine: specific inhibitor of autophagic/lysosomal protein degradation in isolated rat hepatocytes. *Proceedings of the National Academy of Sciences of the United States of America* 79:1889-92
64. Seibenhener ML, Babu JR, Geetha T, Wong HC, Krishna NR, Wooten MW. 2004. Sequestosome 1/p62 is a polyubiquitin chain binding protein involved in ubiquitin proteasome degradation. *Mol Cell Biol* 24:8055-68

65. Seok J, Warren HS, Cuenca AG, Mindrinos MN, Baker HV, et al. 2013. Genomic responses in mouse models poorly mimic human inflammatory diseases. *Proceedings of the National Academy of Sciences of the United States of America* 110:3507-12
66. Shambharkar PB, Blonska M, Pappu BP, Li H, You Y, et al. 2007. Phosphorylation and ubiquitination of the IkappaB kinase complex by two distinct signaling pathways. *EMBO J* 26:1794-805
67. Shegokar R, Al Shaal L, Mishra PR. 2011. SiRNA delivery: challenges and role of carrier systems. *Pharmazie* 66:313-8
68. Shi C-S, Shenderov K, Huang N-N, Kabat J, Abu-Asab M, et al. 2012. Activation of autophagy by inflammatory signals limits IL-1[beta] production by targeting ubiquitinated inflammasomes for destruction. *Nat Immunol* 13:255-63
69. Shi CS, Shenderov K, Huang NN, Kabat J, Abu-Asab M, et al. 2012. Activation of autophagy by inflammatory signals limits IL-1beta production by targeting ubiquitinated inflammasomes for destruction. *Nat Immunol* 13:255-63
70. Shoji-Kawata S, Sumpter R, Leveno M, Campbell GR, Zou Z, et al. 2013. Identification of a candidate therapeutic autophagy-inducing peptide. *Nature* 494:201-6
71. Skaug B, Jiang X, Chen ZJ. 2009. The role of ubiquitin in NF-kappaB regulatory pathways. *Annu Rev Biochem* 78:769-96
72. Smith-Garvin JE, Koretzky GA, Jordan MS. 2009. T cell activation. *Annu Rev Immunol* 27:591-619
73. Snow AL, Xiao W, Stinson JR, Lu W, Chaigne-Delalande B, et al. 2012. Congenital B cell lymphocytosis explained by novel germline CARD11 mutations. *The Journal of experimental medicine* 209:2247-61
74. Staal J, Driege Y, Bekaert T, Demeyer A, Muyllaert D, et al. 2011. T-cell receptor-induced JNK activation requires proteolytic inactivation of CYLD by MALT1. *The EMBO Journal* 30:1742-52
75. Thome M, Charton JE, Pelzer C, Hailfinger S. 2010. Antigen receptor signaling to NF-kappaB via CARMA1, BCL10, and MALT1. *Cold Spring Harbor perspectives in biology* 2:a003004
76. Thome M, Charton JE, Pelzer C, Hailfinger S. 2010. Antigen receptor signaling to NF-kappaB via CARMA1, BCL10, and MALT1. *Cold Spring Harb Perspect Biol* 2:a003004
77. Vallabhapurapu S, Karin M. 2009. Regulation and function of NF-kappaB transcription factors in the immune system. *Annual review of immunology* 27:693-733
78. Vallabhapurapu S, Karin M. 2009. Regulation and function of NF-kappaB transcription factors in the immune system. *Annu Rev Immunol* 27:693-733
79. Wegener E, Oeckinghaus A, Papadopoulou N, Lavitas L, Schmidt-Supprian M, et al. 2006. Essential role for IkappaB kinase beta in remodeling Carma1-Bcl10-Malt1 complexes upon T cell activation. *Mol Cell* 23:13-23
80. Wilcox D, Mason RW. 1992. Inhibition of cysteine proteinases in lysosomes and whole cells. *Biochem J* 285 (Pt 2):495-502

81. Wu CJ, Ashwell JD. 2008. NEMO recognition of ubiquitinated Bcl10 is required for T cell receptor-mediated NF-kappaB activation. *Proc Natl Acad Sci U S A* 105:3023-8
82. Wu CJ, Ashwell JD. 2008. NEMO recognition of ubiquitinated Bcl10 is required for T cell receptor-mediated NF-kappaB activation. *Proc Natl Acad Sci U S A* 105:3023-8
83. Wu CJ, Conze DB, Li T, Srinivasula SM, Ashwell JD. 2006. Sensing of Lys 63-linked polyubiquitination by NEMO is a key event in NF-kappaB activation [corrected]. *Nat Cell Biol* 8:398-406
84. Wu R, Forget MA, Chacon J, Bernatchez C, Haymaker C, et al. 2012. Adoptive T-cell therapy using autologous tumor-infiltrating lymphocytes for metastatic melanoma: current status and future outlook. *Cancer J* 18:160-75
85. Zanin-Zhorov A, Ding Y, Kumari S, Attur M, Hippen KL, et al. 2010. Protein kinase C-theta mediates negative feedback on regulatory T cell function. *Science* 328:372-6
86. Zanin-Zhorov A, Dustin ML, Blazar BR. 2011. PKC-theta function at the immunological synapse: prospects for therapeutic targeting. *Trends Immunol* 32:358-63
87. Zeng H, Di L, Fu G, Chen Y, Gao X, et al. 2007. Phosphorylation of Bcl10 negatively regulates T-cell receptor-mediated NF-kappaB activation. *Mol Cell Biol* 27:5235-45
88. Zhi H, Yang L, Kuo YL, Ho YK, Shih HM, Giam CZ. 2011. NF-kappaB hyper-activation by HTLV-1 tax induces cellular senescence, but can be alleviated by the viral anti-sense protein HBZ. *PLoS pathogens* 7:e1002025
89. Zhi H, Yang L, Kuo YL, Ho YK, Shih HM, Giam CZ. 2011. NF-kappaB hyper-activation by HTLV-1 tax induces cellular senescence, but can be alleviated by the viral anti-sense protein HBZ. *PLoS Pathog* 7:e1002025